

คุณลักษณะและสมบัติการเร่งปฏิกิริยาของตัวเร่งปฏิกิริยา AgLi/SiO<sub>2</sub> บนตัวรองรับซิลิกาที่ต่างกัน  
สำหรับออกซิเดทีพีดีไฮโดรจิเนชันของเอทานอลเป็นอะซีตัลดีไฮด์



นายณรรวิชญ์ มุกดา

จุฬาลงกรณ์มหาวิทยาลัย

บทคัดย่อและแฟ้มข้อมูลฉบับเต็มของวิทยานิพนธ์ตั้งแต่ปีการศึกษา 2554 ที่ให้บริการในคลังปัญญาจุฬาฯ (CUIR)  
เป็นแฟ้มข้อมูลของนิสิตเจ้าของวิทยานิพนธ์ ที่ส่งผ่านทางบัณฑิตวิทยาลัย

The abstract and full text of theses from the academic year 2011 in Chulalongkorn University Intellectual Repository (CUIR)  
are the thesis authors' files submitted through the University Graduate School.

วิทยานิพนธ์นี้เป็นส่วนหนึ่งของการศึกษาตามหลักสูตรปริญญาวิศวกรรมศาสตรมหาบัณฑิต

สาขาวิชาวิศวกรรมเคมี ภาควิชาวิศวกรรมเคมี

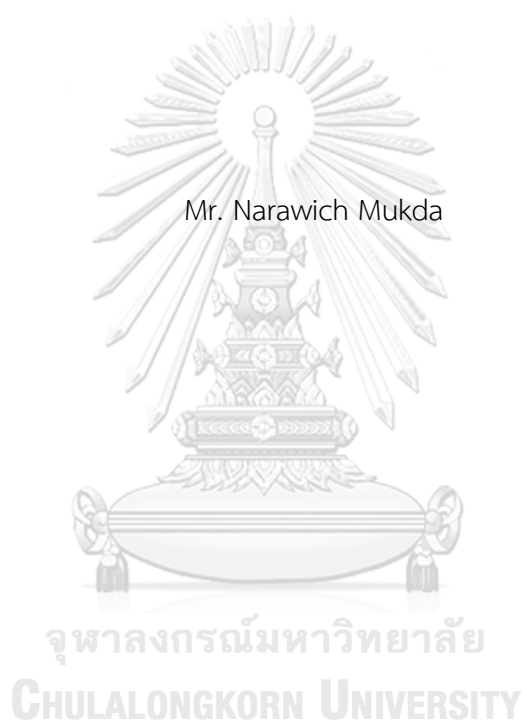
คณะวิศวกรรมศาสตร์ จุฬาลงกรณ์มหาวิทยาลัย

ปีการศึกษา 2560

ลิขสิทธิ์ของจุฬาลงกรณ์มหาวิทยาลัย

CHARACTERISTICS AND CATALYTIC PROPERTIES OF AgLi/SiO<sub>2</sub> CATALYSTS ON DIFFERENT SILICA SUPPORTS FOR OXIDATIVE DEHYDROGENATION OF ETHANOL TO ACETALDEHYDE

YDE



A Thesis Submitted in Partial Fulfillment of the Requirements  
for the Degree of Master of Engineering Program in Chemical Engineering

Department of Chemical Engineering

Faculty of Engineering

Chulalongkorn University

Academic Year 2017

Copyright of Chulalongkorn University

Thesis Title CHARACTERICISTICS AND CATALYTIC PROPERTIES OF  
AgLi/SiO<sub>2</sub> CATALYSTS ON DIFFERENT SILICA  
SUPPORTS FOR OXIDATIVE DEHYDROGENATION  
OF ETHANOL TO ACETALDEHYDE  
By Mr. Narawich Mukda  
Field of Study Chemical Engineering  
Thesis Advisor Professor Bunjerd Jongsomjit, Ph.D.

---

Accepted by the Faculty of Engineering, Chulalongkorn University in Partial  
Fulfillment of the Requirements for the Master's Degree

.....Dean of the Faculty of Engineering  
(Associate Professor Supot Teachavorasinskun, Ph.D.)

THESIS COMMITTEE

.....Chairman  
(Professor Muenduen Phisalaphong, Ph.D.)

.....Thesis Advisor  
(Professor Bunjerd Jongsomjit, Ph.D.)

.....Examiner  
(Chutimon Satirapipathkul, Ph.D.)

.....External Examiner  
(Sasiradee Jantasee, Ph.D.)

นราวิชญ์ มุกดา : คุณลักษณะและสมบัติการเร่งปฏิกิริยาของตัวเร่งปฏิกิริยา AgLi/SiO<sub>2</sub> บนตัวรองรับซิลิกาที่ต่างกันสำหรับออกซิเดทีฟไฮโดรจิเนชันของเอทานอลเป็นอะซีตัลดีไฮด์ (CHARACTERISTICS AND CATALYTIC PROPERTIES OF AgLi/SiO<sub>2</sub> CATALYSTS ON DIFFERENT SILICA SUPPORTS FOR OXIDATIVE DEHYDROGENATION OF ETHANOL TO ACETALDEHYDE) อ.ที่ปรึกษาวิทยานิพนธ์หลัก: ศ. ดร. บรรเจิด จงสมจิตร, 60 หน้า.

งานนี้ให้ความสนใจกับการตรวจสอบของออกซิเดทีฟไฮโดรจิเนชันและนอนออกซิเดทีฟไฮโดรจิเนชันของเอทานอลบนตัวเร่งปฏิกิริยา AgLi/SiO<sub>2</sub> เพื่อผลิตอะซีตัลดีไฮด์โดยมีตัวรองรับซิลิกาที่แตกต่างกัน 3 ชนิด คือ ซิลิกาอนุภาคกลม (อนุภาคขนาดเล็ก; SPS) ซิลิกาอนุภาคขนาดกลาง (MPS) และ ซิลิกาอนุภาคขนาดใหญ่ (LPS) ซิลิกาอนุภาคกลมถูกสังเคราะห์โดยใช้วิธีโซลเจล แต่ทว่า ซิลิกาอนุภาคขนาดกลาง และ ซิลิกาอนุภาคขนาดใหญ่ถูกได้รับจากผู้จัดหาทางการค้า ตัวเร่งปฏิกิริยา AgLi/SiO<sub>2</sub> ถูกเตรียมโดยวิธีการฝังเคลือบแบบเปียกร่วมกัน คุณสมบัติทางเคมีฟิสิกส์ของตัวเร่งปฏิกิริยาถูกวิเคราะห์ด้วยเทคนิคต่าง ๆ เช่น X-ray diffraction (XRD), N<sub>2</sub>-physisorption, SEM-EDX, UV-visible spectroscopy, H<sub>2</sub> Temperature-programmed reduction (H<sub>2</sub>-TPR) ยิ่งกว่านั้นคุณสมบัติความเป็นเบสของตัวเร่งปฏิกิริยาถูกยืนยันด้วยเทคนิค CO<sub>2</sub> Temperature-programmed desorption (CO<sub>2</sub>-TPD) ความว่องไวการเร่งปฏิกิริยา (catalytic activity) และ การกระจายตัวของผลิตภัณฑ์ถูกทดสอบโดยการทำนอนออกซิเดทีฟและออกซิเดทีฟไฮโดรจิเนชันของเอทานอลในวัฏภาคแก๊ส ปฏิกิริยาถูกดำเนินงานภายใต้ความดันบรรยากาศพร้อมด้วยช่วงอุณหภูมิ 200-400 องศาเซลเซียส มันถูกพบว่าตัวเร่งปฏิกิริยา AgLi/SiO<sub>2</sub>-SPS แสดงถึงค่าร้อยละการเปลี่ยนแปลงเอทานอลสูงที่สุด (58.35%) และ ร้อยละการเกิดผลผลิตอะซีตัลดีไฮด์ (56.89%) ที่อุณหภูมิ 400 องศาเซลเซียสสำหรับนอนออกซิเดทีฟไฮโดรจิเนชัน ยิ่งไปกว่านั้นค่าความเป็นเบสของตัวเร่งปฏิกิริยาเป็นอิทธิพลที่โดดเด่นสำหรับปฏิกิริยานี้ ในทางตรงกันข้ามตัวเร่งปฏิกิริยา

ภาควิชา วิศวกรรมเคมี

ลายมือชื่อนิสิต .....

สาขาวิชา วิศวกรรมเคมี

ลายมือชื่อ อ.ที่ปรึกษาหลัก .....

ปีการศึกษา 2560

# # 5970213021 : MAJOR CHEMICAL ENGINEERING

KEYWORDS: OXIDATIVE DEHYDROGENATION, ETHANOL, SILVER, LITHIUM, ACETALDEHYDE

NARAWICH MUKDA: CHARACTERISTICS AND CATALYTIC PROPERTIES OF AgLi/SiO<sub>2</sub> CATALYSTS ON DIFFERENT SILICA SUPPORTS FOR OXIDATIVE DEHYDROGENATION OF ETHANOL TO ACETALDEHYDE. ADVISOR: PROF. BUNJERD JONGSOMJIT, Ph.D., 60 pp.

This work focuses on investigation of the oxidative dehydrogenation and non-oxidative dehydrogenation of ethanol over AgLi/SiO<sub>2</sub> catalysts to produce acetaldehyde by having three different types of silica support, spherical silica particle (small particle size; SPS), medium silica particle size (MPS), and large silica particle size (LPS). The spherical silica particle (SSP) was synthesized using the sol-gel method, whereas SiO<sub>2</sub> (MPS) and SiO<sub>2</sub> (LPS) were obtained from commercial suppliers. AgLi/SiO<sub>2</sub> catalysts were prepared by incipient wetness co-impregnation method. The physicochemical properties of catalysts were analyzed by using several technique such as X-ray diffraction (XRD), N<sub>2</sub>-physisorption, SEM-EDX, UV-visible spectroscopy, H<sub>2</sub>-TPR. Moreover, the basicity properties of catalysts were confirmed by CO<sub>2</sub> Temperature-programmed desorption (CO<sub>2</sub>-TPD) technique. The catalytic activity and product distribution were tested by performing both non-oxidative and oxidative dehydrogenation of gas phase ethanol. The reactions were operated at atmospheric pressure with the temperature range of 200-400 °C. It was found that the AgLi/SiO<sub>2</sub>-SPS catalyst exhibited the highest ethanol conversion (58.35%) and acetaldehyde yield (56.89%) at the temperature of 400 °C for non-oxidative dehydrogenation. In addition, the basicity of catalyst play a strong influence for this reaction. In contrast, the AgLi/SiO<sub>2</sub>-LPS catalyst exhibited the highest acetaldehyde yield (76.81%) at the temperature of 300 °C for the oxidative dehydrogenation because its higher Ag<sup>δ+</sup> clusters and Ag<sup>0</sup> species due to its high reducibility.

Department: Chemical Engineering      Student's Signature .....

Field of Study: Chemical Engineering      Advisor's Signature .....

Academic Year: 2017

## ACKNOWLEDGEMENTS

The author would like to express the gratefulness and appreciation to his advisor, Professor Dr. Bunjerd Jongsomjit for his best suggestion, useful knowledge and counsel, and invaluable encouragement along this research. This thesis would not be have been completed without all the support and guidance that the author has always received from his advisor, In addition, he is also grateful to thank Professor Dr. Muenduen Phisalaphong, as the chairman of the thesis committee, Dr. Chutimon Satirapipathkul, Dr. Sasiradee Jantasee, and Dr. Jakrapan Janlamool for their dedicated in spending the time for his research suggestion.

Moreover, the author thank the Grant for International Research Integration: Chula Research Scholar, Ratchadaphiseksomphot Endowment Fund for financial support of this project.



จุฬาลงกรณ์มหาวิทยาลัย  
CHULALONGKORN UNIVERSITY

## CONTENTS

	Page
THAI ABSTRACT .....	iv
ENGLISH ABSTRACT .....	v
ACKNOWLEDGEMENTS .....	vi
CONTENTS .....	vii
LIST OF FIGURES .....	viii
LIST OF TABLE .....	x
Chapter 1 Introduction .....	1
1.1 Introduction .....	1
1.2 Objective .....	4
1.3 Research Scope .....	4
1.4 Research methodology .....	5
Chapter 2 Background and literature review .....	6
CHAPTER 3 .....	14
EXPERIMENT .....	14
3.4 Research plan .....	21
3.5 Expected benefits .....	21
Chapter 4 Results and discussion .....	22
Chapter 5 CONCLUSIONS AND RECOMMENDATIONS .....	45
REFERENCES .....	47
VITA .....	60

## LIST OF FIGURES

<b>Figure 1.1</b> organic products from ethanol.....	1
<b>Figure 1.2</b> The demand forecasting of acetaldehyde during 2017-2022.....	2
<b>Figure 1.3</b> The mechanism for ethanol dehydrogenation over Ag/SiO <sub>2</sub> .....	3
<b>Figure 2.1</b> The mechanism for ethanol oxidative dehydrogenation over Ag/SiO <sub>2</sub> .....	7
<b>Figure 2.2</b> pathway for oxidative dehydrogenation over silver-based catalyst .....	8
<b>Figure 2.3</b> global production of acetaldehyde.....	10
<b>Figure 2.4</b> global acetaldehyde consumption in 2016.....	11
<b>Figure 3.1</b> Catalytic reaction system of oxidative dehydrogenation.....	18
<b>Figure 3.2</b> Catalytic reaction system of dehydrogenation.....	20
<b>Figure 4.1</b> XRD patterns of silica support .....	22
<b>Figure 4.2</b> XRD patterns of silver lithium supported on silica supports.....	23
<b>Figure 4.3</b> The SEM images of catalysts .....	24
<b>Figure 4.4</b> EDX mapping for AgLi/SiO <sub>2</sub> -SPS.....	15
<b>Figure 4.5</b> EDX mapping for AgLi/SiO <sub>2</sub> -MPS.....	16
<b>Figure 4.6</b> EDX mapping for AgLi/SiO <sub>2</sub> -LPS.....	16
<b>Figure 4.7</b> The UV-visible spectra of all catalysts.....	29
<b>Figure 4.8</b> CO <sub>2</sub> -TPD profiles of catalysts.....	30
<b>Figure 4.9</b> TPR profiles of catalysts.....	31
<b>Figure 4.10</b> Relation between ethanol conversion and temperature .....	33
<b>Figure 4.11</b> Relation between acetaldehyde selectivity and temperature for all catalyst .....	34
<b>Figure 4.12</b> Relation between product selectivity and temperature for AgLi/SiO <sub>2</sub> -SPS catalyst .....	35



<b>Figure 4.13</b> Relation between product selectivity and temperature for AgLi/SiO <sub>2</sub> -MPS catalyst .....	35
<b>Figure 4.14</b> Relation between product selectivity and temperature for AgLi/SiO <sub>2</sub> -MPS catalyst .....	36
<b>Figure 4.15</b> Relation between acetaldehyde yield and temperature for all catalysts .....	37
<b>Figure 4.16</b> Ethanol conversion of all catalysts for oxidative dehydrogenation reaction. ....	39
<b>Figure 4.17</b> Relation between acetaldehyde selectivity and temperature for all catalysts.....	40
<b>Figure 4.18</b> Relation between product selectivity and temperature for AgLi/SiO <sub>2</sub> -SPS catalyst.....	41
<b>Figure 4.19</b> Relation between product selectivity and temperature for AgLi/SiO <sub>2</sub> -MPS catalyst.....	41
<b>Figure 4.20</b> Relation between product selectivity and temperature for AgLi/SiO <sub>2</sub> -LPS catalyst.....	42
<b>Figure 4.21</b> acetaldehyde yield of all catalysts for oxidative dehydrogenation reaction. ....	43
<b>Figure B.1</b> The calibration curve of ethanol. ....	54
<b>Figure B.2</b> The calibration curve of acetaldehyde.....	54
<b>Figure B.3</b> The calibration curve of ethylene.....	55
<b>Figure B.4</b> The calibration curve of diethyl ether.....	55
<b>Figure B.5</b> The calibration curve of carbon monoxide.....	56
<b>Figure B.6</b> The calibration curve of carbon dioxide.....	56
<b>Figure C.1</b> The calibration curve of carbon dioxide obtained from CO <sub>2</sub> – TPD profiles.....	57

## LIST OF TABLE

<b>Table 2.1</b> Physical properties of acetaldehyde.....	9
<b>Table 3.1</b> Research plan.....	21
<b>Table 4.1</b> the elemental concentration of supports and catalysts determined by EDX.....	27
<b>Table 4.2</b> The physical properties of SiO <sub>2</sub> and AgLi/SiO <sub>2</sub> catalysts .....	28
<b>Table 4.3</b> The amounts of basic sites of catalysts.....	31
<b>Table 4.4</b> The catalytic activity of all catalysts for non-oxidative dehydrogenation.....	38
<b>Table 4.5</b> The catalytic activity of all catalysts for oxidative dehydrogenation .....	44
<b>Table B1</b> Retention times of reactant for FID and TCD gas chromatography .....	53

## CHAPTER 1

### INTRODUCTION

#### 1.1 Introduction

Due to the high prices of crude oil and natural gas. The use of alternative resources must be more focused on. Bio-ethanol is one of the most interesting alternative raw materials that can be produced by the fermentation of molasses, tapioca and other renewable resources. There are many products that can be produced from ethanol, for example, ethylene, diethyl ether, ethyl acetate, ethane, hydrogen, and acetaldehyde (which in turn is an intermediate in producing acetic acid, ethyl acetate, butyraldehyde, crotonaldehyde, and n-butanol). The products obtained from ethanol are shown in **Figure 1.1**.

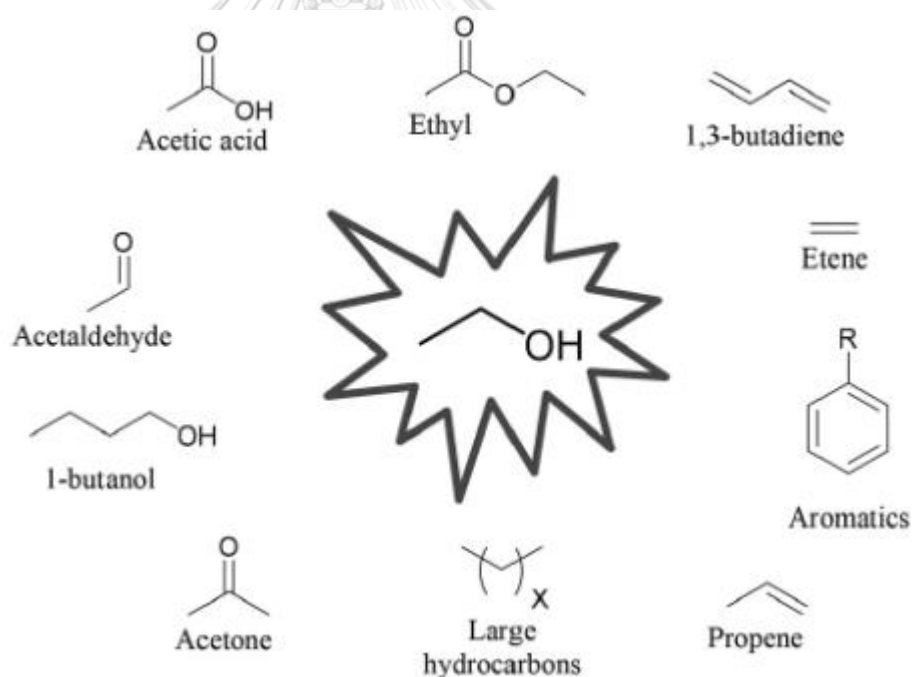


**Figure 1.1** organic products from ethanol

Nowadays, acetaldehyde is mostly used in petrochemical industry for the preparation of pyridines derivatives, acetic acid, vinyl acetate, and useful resin. Acetaldehyde can be produced from dehydrogenation and oxidative dehydrogenation reaction of ethanol. In addition, the demand for acetaldehyde is in an increasing trend during

2017-2022 [1] as shown in **Figure 1.2**. The use of oxidative dehydrogenation of ethanol with  $O_2$  (friendly oxidant) on various heterogeneous catalysts is to achieve the environmental and economic acceptability due to it can avoid the use of large excess of toxic and expensive metal-based oxidants.

**Global Acetaldehyde Market: Volume (In Kilo Tons), 2015-2022**

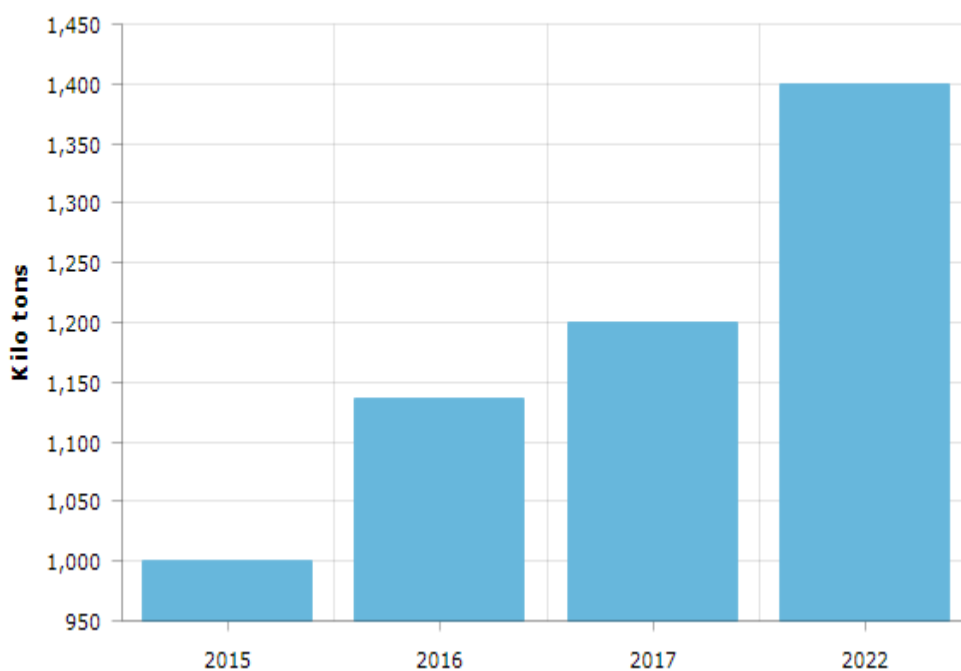


**Figure 1.2** The demand forecasting of acetaldehyde during the period of 2017-2022. [1]

In general, silica-supported catalyst is one of the most popular supports to use as the support for the silver catalyst in the reaction of oxidative dehydrogenation because of its high activity even the content of the metal is low. Spherical silica particle (SSP) is one type of silica that has the appropriate properties to be a great support such as their pore size distribution, thermal stability, and high surface area. In addition, silica-supported silver catalyst gives a benefit on the oxygen content, which is an efficient heterogeneous catalyst for the oxidant-free dehydrogenation of ethanol into acetaldehyde.

The Ag-based catalyst has been used on various supports and given the high activity in the dehydrogenation of alcohols [2]. When the silica is used as the support of the Ag-based catalyst, after the  $H_2$  and acetaldehyde are desorbed from the catalyst, the catalyst will regenerate itself as shown in **Figure 1.3**.

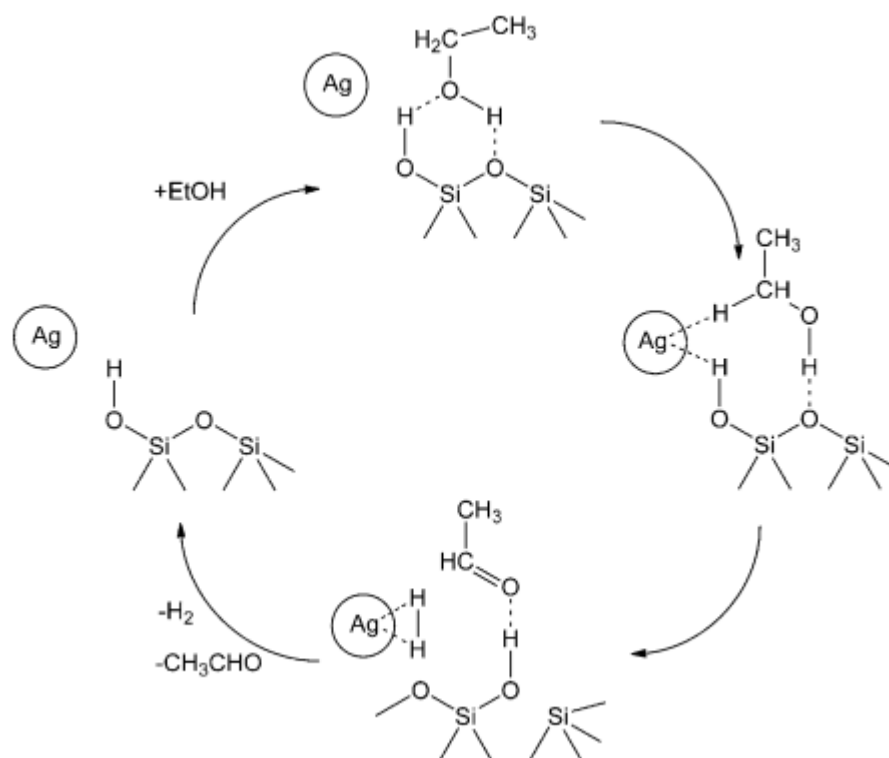


**Figure 1.3** The mechanism for ethanol dehydrogenation over Ag/SiO<sub>2</sub> [2]

Furthermore, there is another way to develop the silica-supported silver catalyst to be more basic by adding the Li<sub>2</sub>O since when the lithium content is increased, the surface acidity will be decreased [3].

In this research, the oxidative dehydrogenation of ethanol over AgLi/SiO<sub>2</sub> catalysts having different types of silica supports to produce acetaldehyde will be investigated. Firstly, the spherical silica particle will be synthesized by sol-gel method. Then, the AgLi/SiO<sub>2</sub> catalysts will be prepared by using incipient wetness impregnation technique. Secondly, the characteristics of the catalyst will be measured by various techniques such as XRD, N<sub>2</sub>-physisorption, UV-visible, TPR, SEM-EDX, and CO<sub>2</sub>-TPD. Lastly,

dehydrogenation reaction of ethanol will be performed to test the catalytic activity and product distribution.

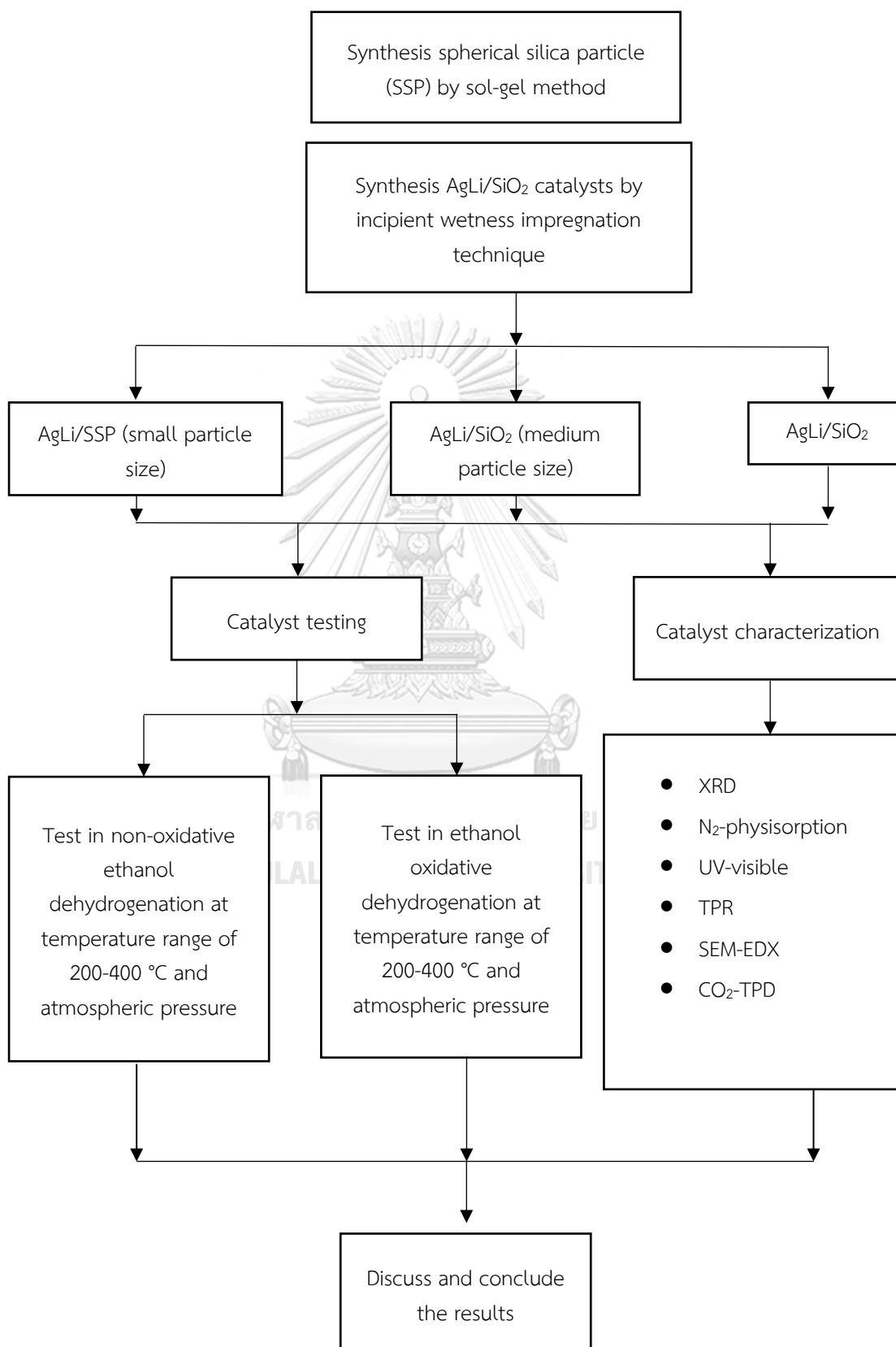
## 1.2 Objective

This work aims to investigate the oxidative dehydrogenation of ethanol over AgLi/SiO<sub>2</sub> catalysts to produce acetaldehyde. The study focuses on the activity of catalyst by varying the types of silica and the reaction with/without oxygen (oxidative dehydrogenation and dehydrogenation, respectively).

## 1.3 Research Scope

1. Preparation of spherical silica particle (SSP) by sol-gel method
2. Loading the metals (silver and lithium) via incipient wetness impregnation method onto the different types of silica support (SSP and 2 commercial silica supports)
3. Analyzing the physiochemical properties of catalysts with several techniques; XRD, N<sub>2</sub>-physisorption (BET, BJH), UV-visible, H<sub>2</sub>-TPR, SEM-EDX and basicity properties via CO<sub>2</sub>-TPD techniques.
4. Reaction test of the catalysts for ethanol in both oxidative dehydrogenation and dehydrogenation, which are both carried out in a fixed-bed reactor under atmospheric pressure and temperature range of 200-400 °C.

## 1.4 Research methodology



## CHAPTER 2

### BACKGROUND AND LITERATURE REVIEW

This project would like to investigate the dehydrogenation of ethanol to acetaldehyde by using the heterogeneous catalysts to drive the reaction. The catalysts used in this project are composed of silica as the support. Then, loading the metal including silver and lithium to improve the activity and selectivity to produce the desired product. In this part, the basic knowledge of ethanol, acetaldehyde, and development of catalyst to convert ethanol to acetaldehyde will be explained.

#### 2.1 Ethanol

Ethanol is a renewable fuel and plays important role in both chemical and energy industries. Ethanol can be produced easily via fermentation of renewable sources such as corn, sugarcane, or other biomass waste. This is called bio-ethanol. As mentioned in previous part, acetaldehyde can be produced from ethanol, there are 2 main reactions that mostly used in this process, which are oxidation reaction and dehydrogenation reaction.

##### 2.1.1 Oxidation reaction of ethanol

Oxidation reaction of alcohols is usually used to make ketones, carboxylic acids, and aldehydes (which is focused in this project). In this process, vapor phase ethanol will be oxidized catalytically with oxygen.

Partial oxidation to acetaldehyde is the use of an excess of ethanol, then separate the acetaldehyde as soon as it forms.



At present, there are many researches try to find out a better way to produce the acetaldehyde from ethanol by using a various type of supported metal catalyst such as gold[4], nickel[5], palladium[6], or copper[7]. Besides, there are many properties that affect the performance of catalyst such as particle size of catalyst and acid-base of the support.



Moreover, these supported metal catalysts is good in activity for aerobic or oxidative dehydrogenation of ethanol.

There are many researchers study about the oxidative dehydrogenation. They found that the use of oxygen as co-feed give the higher performance of catalyst activity since the oxygen atoms were adsorbed on the active metal of catalyst then the oxygen oxidized the  $\text{Ag}^0$  to  $\text{Ag}^{\delta+}$  that more active in oxidative dehydrogenation reaction. In this case, the main product is acetaldehyde and  $\text{H}_2\text{O}$  will be obtained as by-product instead of  $\text{H}_2$  compared to non-oxidative dehydrogenation reaction [8, 9].

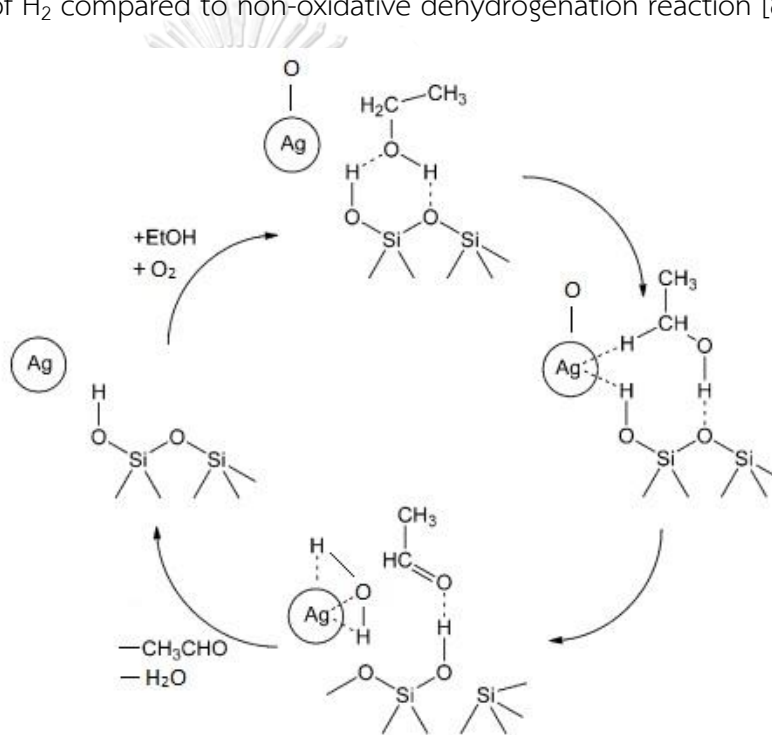


**Figure 2.1** The mechanism for ethanol oxidative dehydrogenation over  $\text{Ag}/\text{SiO}_2$

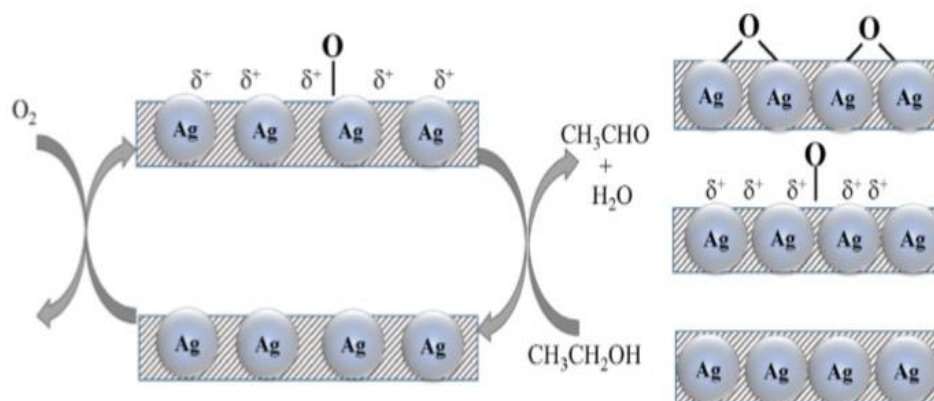


**Figure 2.2** pathway for oxidative dehydrogenation over silver-based catalyst [9]

### 2.1.2 Dehydrogenation reaction of ethanol

Dehydrogenation reaction is the reaction that is conducted to remove a hydrogen from the reactant's molecule. This reaction is an endothermic reaction occurring at temperature higher than 100 °C. Acetaldehyde from this reaction will be focused as the main product that can be separated by condensation and hydrogen can also be produced.



During dehydrogenation reaction undergoes, hydrogen will be removed from the reactant by nucleophile addition of basic catalysts. The product activity and selectivity depend on the kind of catalyst and external conditions such as pressure, temperature, or retention time.

### 2.2 Acetaldehyde

Acetaldehyde (also known as ethyl aldehyde or ethanal) is a colorless, flammable liquid or gas with a specific odor. It is an important, highly reactive aldehyde, mainly used as a starting material in the synthesis of n-butyl alcohol, ethyl acetate, perfumes, aniline dyes, plastic, rubber, and other useful chemical compounds. Moreover, acetaldehyde is also an

intermediate in the metabolism of alcohol. Large amounts of acetaldehyde may cause death from respiratory paralysis. Small amounts of acetaldehyde are produced naturally through gut microbial fermentation. Acetaldehyde has been shown to increase the risk of developing cirrhosis of the liver, multiple forms of cancer, and alcoholism.

Since acetaldehyde is a highly reactive aldehyde, it is often used in a commercial process. Acetaldehyde is not only an intermediate of the product, but also a solvent. Whereas, when the reaction temperature is reached to more than 420 °C, acetaldehyde will be composed into methane and carbon monoxide[10].

From the dangerous properties of acetaldehyde, the safety information of acetaldehyde should be focused. From the Gas Data Book, the lower and upper explosive limits of acetaldehyde are 4% by volume and 60% by volume, respectively.

**Table 2.1** Physical properties of acetaldehyde

Properties	Information
Molecular weight	44.053 g/mol
Normal boiling point	20.8 °C
Normal melting point	-123.5 °C
Vapor pressure	740 mmHg @20 °C
Relative vapor density	1.52 (air = 1)
Flash point temperature	-38.0 °C
Ignition temperature	175 °C

### 2.2.1 Acetaldehyde production

Acetaldehyde was first observed in 1774 by Carl Wilhelm Scheele during the reaction of black manganese dioxide and sulfuric acid with alcohol [10]. Finally, pure acetaldehyde can be produced in 1835 by

Liebig via the oxidation of ethanol with chromic acid and designated this product “aldehyde”. After that, name “aldehyde” was changed to “acetaldehyde”, a contraction of the term “alcohol dehydrogenatus”

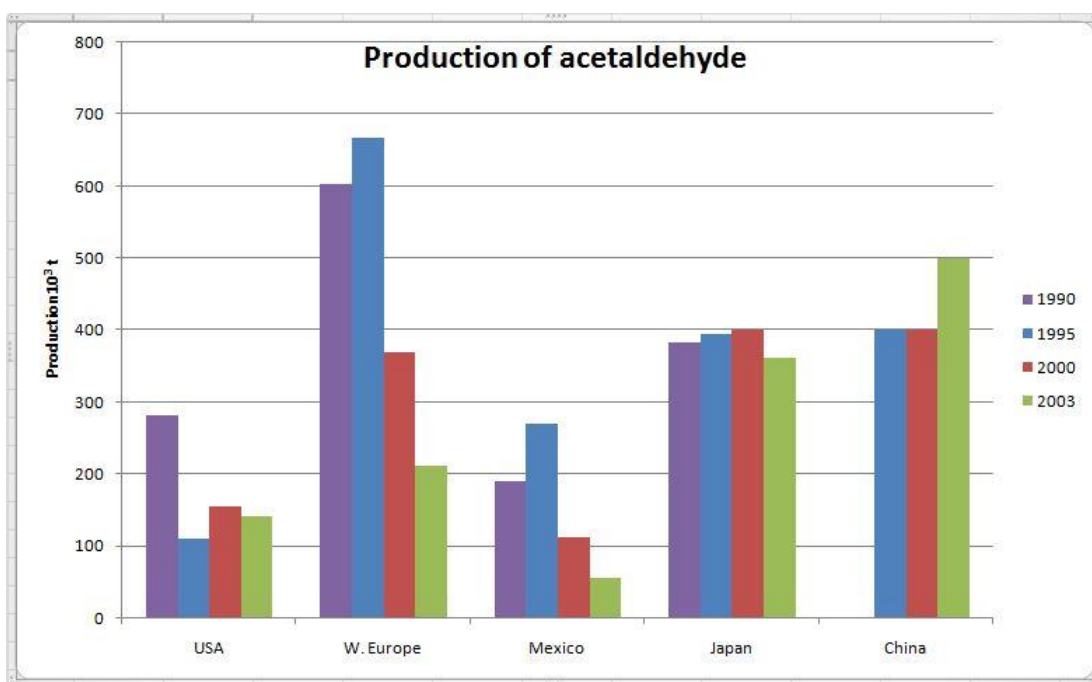
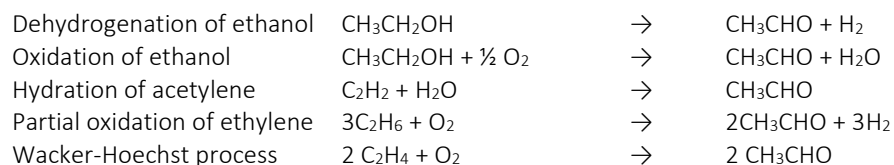


Figure 2.3 global production of acetaldehyde

Acetaldehyde can be produced from many commercial processes including the dehydrogenation and oxidation of ethanol [11, 12], the hydration of acetylene [13], the partial oxidation of hydrocarbons, and the Wacker-Hoechst process [14]. The equations of these reactions are shown below:



### 2.2.2 Acetaldehyde applications and market trend

The mostly use of acetaldehyde is as the starting material in the production of chemical goods such as n-butyl alcohol, ethyl acetate, perfumes, aniline dyes, plastic, rubber, and other useful chemical compounds.

From Chemical Economics Handbook, pyridines, pentaerythritol, acetic acid, and acetate esters are 34%, 23%, 18%, and 10% of global acetaldehyde consumption in 2016, respectively. Other applications of acetaldehyde accounted for the remaining 15% of global acetaldehyde consumption in 2016.

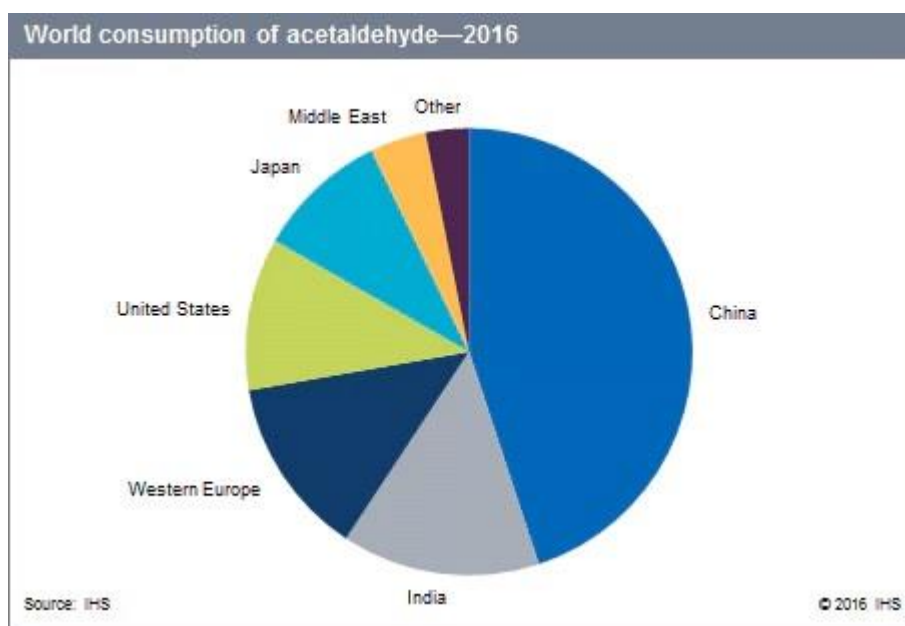


**Figure 2.4** global acetaldehyde consumption in 2016 [15]

From **Figure 2.4**, China is the largest global acetaldehyde consumption in 2016 that is almost half of global acetaldehyde consumption. The main product from acetaldehyde in China are acetic acid, pyridines, and pentaerythritol, which are 28% of total acetaldehyde consumption in China. Furthermore, Chinese acetaldehyde consumption is forecasted to increase by 4% per year through 2021.

While, India accounted 14% of global acetaldehyde consumption in 2016. Pyridines is the main product in this country, 90% of total acetaldehyde consumption is pyridines.

Moreover, the other region in the world has the forecast of acetaldehyde consumption growth about 1 to 2.5% and the average growth of global acetaldehyde consumption is forecast annual rate of 3.0%

### 2.3 Silver-based catalyst

Silver is the group IB transition metal. There are many morphologies of silver-based material such as nanobar, nanocubic, nanosphere etc. that their functions could be applied in many fields especially for heterogeneous catalytic due to its specific physical and chemical structure. The silver-based catalysts have been used in form of a bulk metal or dispersed metal supported on various supports. The performance of silver catalysts depends strongly on their surface structure and surface sites. They are very sensitive to the preparation method, pretreatment, reaction condition, and the size of silver nanoparticles.

The interest in selective oxidative dehydrogenation of alcohols by using silver-based catalyst is continuously growing in commercial process [16]. When compare the silver-based catalyst to other metals, such as platinum, palladium, or nickel, the hydrogen interacts only very weakly with extended silver surfaces and no dissociative chemisorptions could occur at low temperature[17].

Recently, there are researchers found that silver-containing catalysts on the basic or acidic oxides support are very active in non-oxidative dehydrogenation of alcohols [18]. For example, the silica-supported silver catalyst shows the higher efficient heterogeneous catalyst for the non-oxidative dehydrogenation of ethanol into acetaldehyde than supported gold catalysts that is more expensive [19].

In 1978, Wachs et al. [20] published the study of the oxidation of methanol over silver catalyst, there are many steps of methanol oxidation mechanism. Firstly, methoxy formation through the activation of O-H bond by adsorbed atomic oxygen. Secondly, C-H bond cleavage to form formaldehyde and hydrogen. Thirdly, hydrogen atoms at the surface are recombined to form methanol. Lastly, formaldehyde was adsorbed to yield methyl formate and hydrogen by the adsorbed  $\text{H}_2\text{COOCH}_3$  intermediate.

The mechanism steps were shown below;



In the same way, if the methanol was changed into ethanol, when the oxygen is excess, ethanol on Ag catalyst is first oxidized to surface ethoxy and water upon adsorption at 453 °C, and then decomposed to acetaldehyde and hydrogen [21].



## CHAPTER 3

### EXPERIMENT

This chapter will explain about the experimental procedures. There are 3 parts of experimental procedures. First, the silica support and silver lithium catalysts will be prepared. Second, the synthesized catalysts will be characterized. Last, the prepared catalysts will be brought to study the dehydrogenation and oxidative dehydrogenation of ethanol.

#### 3.1 Catalyst preparation

The spherical silica particle (SSP) was prepared by sol-gel method, and then SSP and 2 commercial silica supports were loaded with Ag and Li by the incipient wetness impregnation method.

##### 3.1.1 Chemicals for synthesis of spherical silica particle and AgLi/SiO<sub>2</sub>

1. Tetraethyl orthosilicate (TEOS) 98 wt% available from Aldrich.
2. Ammonia 30 wt% available from Penreac.
3. Ethanol 99.99 wt% available from J. T. Baker.
4. Cetyltrimethylammonium bromide (CTAB) available from Aldrich.
5. Silver (I) nitrate 99 wt% available from Aldrich.
6. Lithium (I) nitrate 98 wt% available from Aldrich.
7. Deionized water

##### 3.1.2 Synthesis of spherical silica particle support

The spherical silica particle support was prepared by sol-gel method as reported by Janlamool J. et al. [22] and Fuchigami K. et al. [23]. First, the synthesized gel was prepared by mixing the composition (molar ratio) of 1TEOS: 0.3 CTAB: 11 NH<sub>3</sub>: 58 ethanol: 144 H<sub>2</sub>O. Then, the mixture was mixed and stirred at room temperature for 2 hours. After that, the precipitate were washed with deionized water and filtrated. After filtration, the precipitate was dried at 110 °C for 12 hours and calcined with air flow at 550 °C for 6 hours. Finally, the spherical silica particle was obtained in form of white powder.



3.1.3 Preparation of silver and lithium loaded on spherical silica particle and commercial silica supports.

In this section, silver and lithium loaded on silica supports was discussed. The AgLi-SiO<sub>2</sub> catalysts were prepared by the incipient wetness co-impregnation method. Silver (I) nitrate and lithium (I) nitrate were mixed as aqueous solution with an optimum composition to obtain 4.7 wt% of Ag and 0.7 wt% of Li on the spherical silica particle and 2 commercial silica supports. After the silver and lithium were loaded on silica supports, they were dried in an oven for 12 hours and calcined in air at 400 °C for 4 hours at the heating rate of 10 °C min<sup>-1</sup>.

### 3.2 Catalyst characterization

#### 3.2.1 X-ray diffraction (XRD)

X-ray diffraction (XRD): Bruker D8 Advance X-ray diffractometer with Cu-K $\alpha$  radiation ( $\lambda = 1.54056 \text{ \AA}$ ) was used to determine the phase composition of catalysts. The spectra were scanned at a rate of 2.4° min<sup>-1</sup> in the  $2\theta$  range of 15 to 80° with resolution 0.04°. The standard peak is pure silica, silver oxide, and lithium oxide.

#### 3.2.2 Nitrogen physisorption

The BET surface area, pore volume and pore size were determined by physisorption of N<sub>2</sub> using a BET and BJH methods. The amounts of catalyst used is 0.05 g for each sample. The instrument is Micromeritics ASAP 2000 automated system. All of samples were degassed at 120 °C in nitrogen flow for 3 hours to remove the moisture and other adsorbates.

#### 3.2.3 UV-visible spectroscopy (UV-vis)

The oxidation state of Ag was determined using UV–visible absorption spectroscopy (Perkin Elmer Lambda-650, wavelength of 200–800 nm with a step size at 1 nm).

#### 3.2.4 Temperature-programmed reduction (TPR)

The reduction behavior of catalysts was evaluated by TPR. 0.1 g of catalyst was used and pretreated at 250 °C under nitrogen flow for 1 hour. The reduction profile was operated at temperature ramping to 500 °C with the rate of 10 °C min<sup>-1</sup> during flowing of 10% H<sub>2</sub> in air.

#### 3.2.5 Scanning electron microscopy (SEM) and energy dispersive X-ray spectroscopy (EDX)

SEM and EDX were used to investigate the morphology and elemental distribution at the surface of the samples by using Hitachi mode S-3400 N. Micrographs were taken at the accelerating voltage of 30 kV and magnification ranging from 1,000 to 10,000 and the resolution of 3 nm. The SEM was operated by using the secondary scattering electron (SE) mode. EDX was performed by using Apollo X Silicon Drift Detector Series by EDAX.

#### 3.2.6 Carbon dioxide Temperature-Programmed Desorption (CO<sub>2</sub>-TPD)

The basicity of catalyst was determined by CO<sub>2</sub>-TPD using a Micromeritics Chemisorp 2750. First, 0.1 g of the catalyst was pretreated at 500 °C with flowing of helium for an hour. Then, the catalyst was saturated with pure CO<sub>2</sub> at 30°C. After saturation, the physisorbed CO<sub>2</sub> was desorbed in a helium flow. Then, the catalyst was heated from 30 to 500 °C with a heating rate of 10 °C/min. The amount of carbon dioxide in effluent was detected via TCD signal as a function of time.

### 3.3 Reaction study in oxidative dehydrogenation and dehydrogenation of ethanol

#### 3.3.1 Oxidative dehydrogenation reaction of ethanol

##### 3.3.1.1 Chemicals for the reaction study

1. Absolute ethanol purity of 99.99% available from Merck.

2. Nitrogen gas ultra-high purity of 99.99% available from Linde.

3. Hydrogen gas ultra-high purity of 99.99% available from Linde.

4. Air zero balance nitrogen available from Linde.

##### 3.3.1.2 Reaction study procedure

Oxidative dehydrogenation of ethanol was studied to determine the catalytic activity and desired product selectivity of the different AgLi-SiO<sub>2</sub> catalysts. Typically, 0.05 g of catalyst was packed below 0.01 g of quartz wool in a middle fixed-bed continuous flow micro-reactor, the reactor is made of a borosilicate glass with an inside diameter of 0.7 cm. Then, the catalyst was preheated at 200 °C for 30 minutes to eliminate the moisture in N<sub>2</sub> carrier gas. After preheated step, it was pre-reduced in situ in flowing H<sub>2</sub> at 300 °C for 1 hour. Ethanol was introduced into the reactor by syringe pump at the volumetric flow rate of 60 mL/min by bubbling N<sub>2</sub> as a carrier gas through the vaporizer at 120 °C (boiling point of ethanol is 60 °C) to maintain the partial pressure of ethanol with WHSV of 22.9 ( $g_{\text{ethanol}}/g_{\text{cat}} \cdot h$ ). Carrier gas (N<sub>2</sub>) flow rate was kept at 60 mL/min. Oxygen was flew into the reactor with other gases since this is an oxidative dehydrogenation reaction. When O<sub>2</sub> was flew with N<sub>2</sub>, the flow rate of N<sub>2</sub> was decreased to 17.8 mL/min and set the flow rate of air to 46 mL/min. Catalytic reaction was operated under the atmospheric pressure and the temperature

range of 200 to 400 °C. The product was detected by using 2 types of gas chromatography techniques including, flame ionization detector (FID) and thermal conductivity detector (TCD). TCD's instrument is Shimadzu GC8A (Porapak-Q and Molecular sieve 5A) that inorganic compositions can be separated. FID's instrument is Shimadzu GC14B (DB-5) was used to separate the light hydrocarbon products.

### 3.3.1.3 Instruments and apparatus

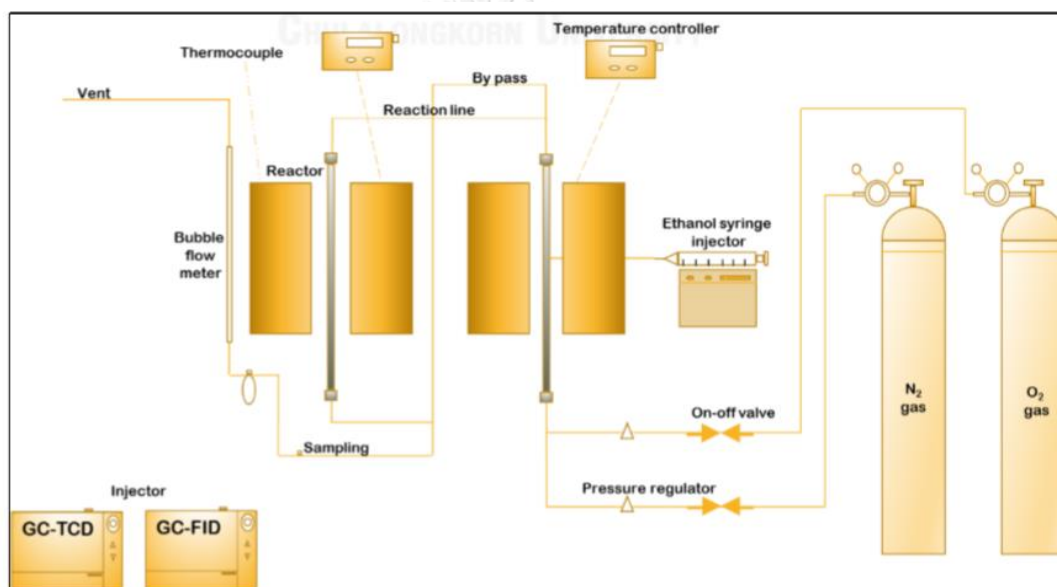


Figure 3.1 Catalytic reaction system of oxidative dehydrogenation

### 3.3.2 Dehydrogenation reaction of ethanol

#### 3.3.2.1 Chemicals for the reaction study

1. Absolute ethanol purity of 99.99% available from Merck.
2. Nitrogen gas ultra-high purity of 99.99% available from Linde.
3. Hydrogen gas ultra-high purity of 99.99% available from Linde.

#### 3.3.2.2 Reaction study procedure

Dehydrogenation of ethanol was studied to determine the catalytic activity and desired product selectivity of the different AgLi-SiO<sub>2</sub> catalysts. Typically, 0.05 g of catalyst was packed below 0.01 g of quartz wool in a middle fixed-bed continuous flow micro-reactor, the reactor is made of a borosilicate glass with an inside diameter of 0.7 cm. Then, the catalyst was preheated at 200 °C for 30 minutes to eliminate the moisture in N<sub>2</sub> carrier gas. After preheated step, it was pre-reduced in situ in flowing H<sub>2</sub> at 300 °C for 1 hour. Ethanol was introduced into the reactor by syringe pump at the volumetric flow rate of 60 mL/min by bubbling N<sub>2</sub> as a carrier gas through the vaporizer at 120 °C (boiling point of ethanol is 60 °C) to maintain the partial pressure of ethanol with WHSV of 22.9 (g<sub>ethanol</sub>/g<sub>cat</sub>·h). Carrier gas (N<sub>2</sub>) flow rate was kept at 60 mL/min. Catalytic reaction was operated under the atmospheric pressure and the temperature range of 200 to 400 °C. The product was detected by using 2 types of gas chromatography techniques including, flame ionization detector (FID) and thermal conductivity detector (TCD). TCD's instrument is Shimadzu GC8A (Porapak-Q and Molecular sieve 5A) that inorganic compositions can be separated. FID's instrument is Shimadzu GC14B (DB-5) was used to separate the light hydrocarbon products.

## 3.3.2.3 Instruments and apparatus

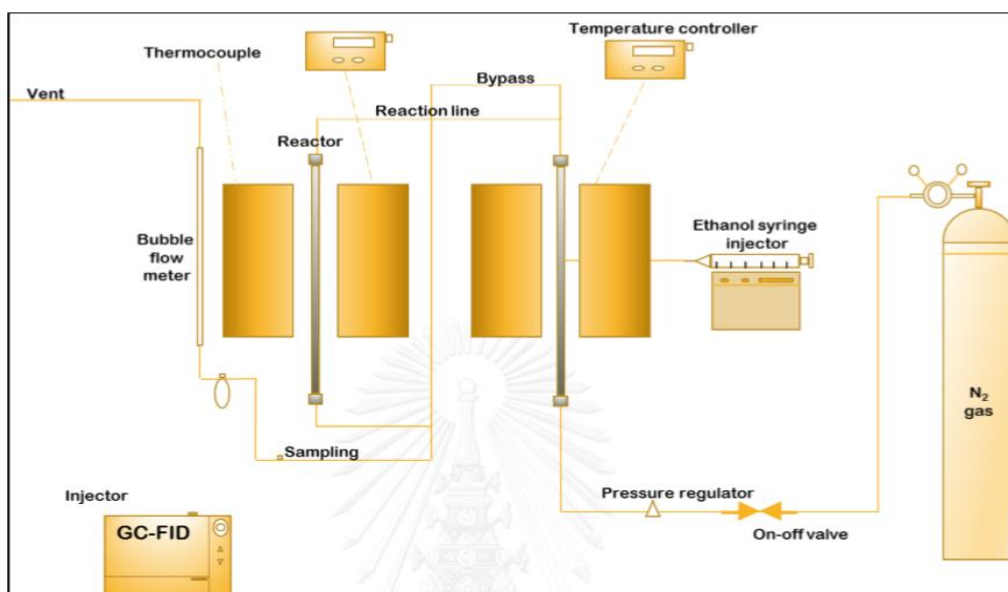


Figure 3.2 Catalytic reaction system of dehydrogenation

### Catalyst nomenclature

The name of catalysts will be based on their silica particle size. First, spherical silica particle that is the smallest particle size (0.6  $\mu\text{m}$ ) will be named as small particle size (SPS). Second, first commercial silica support that its particle size is between SSP and the second commercial silica will be named as medium particle size (MPS). Last, second commercial silica support that its particle size is the biggest will be named as large particle size (LPS).

### 3.4 Research plan

Table 3.1 Research plan

Plan	Year 2560												Year 2561							
	03	04	05	06	07	08	09	10	11	12	01	02	03	04	05	06	07			
Study the theory and literature review	←————→																			
SSP preparation					←————→															
AgLi/SiO <sub>2</sub> (SPS, MPS, LPS) preparation							←————→													
XRD, UV-vis, SEM&EDX							←————→													
BET, CO <sub>2</sub> -TPD, H <sub>2</sub> -TPR										←————→										
Non-oxidative dehydrogenation test									←————→											
Oxidative dehydrogenation test										←————→										
Discussion and conclusion																←————→				

### 3.5 Expected benefits

1. It will decrease the cost of acetaldehyde production.
2. It will obtain the optimum silver lithium catalyst for ethanol dehydrogenation.
3. It will obtain the optimum condition for ethanol dehydrogenation.
4. It can be applied for the real industries in the near future.

## CHAPTER 4

### RESULTS AND DISCUSSION

In this chapter, the characteristics of the catalysts were investigated and explained by several techniques such as X-ray diffraction (XRD),  $N_2$ -physisorption, UV-visible spectroscopy (UV-vis), temperature-programmed reduction ( $H_2$ -TPR), scanning electron microscopy (SEM) and energy dispersive X-ray spectroscopy (EDX), and carbon dioxide temperature-programmed desorption ( $CO_2$ -TPD). In addition, the catalytic studies for both dehydrogenation and oxidative dehydrogenation reactions using fixed bed micro-reactor with temperature ranged from 200 to 400 °C were also discussed in this chapter.

#### 4.1 Catalysts characterization

##### 4.1.1 Physical properties

##### 4.1.1.1 X-ray diffraction (XRD)

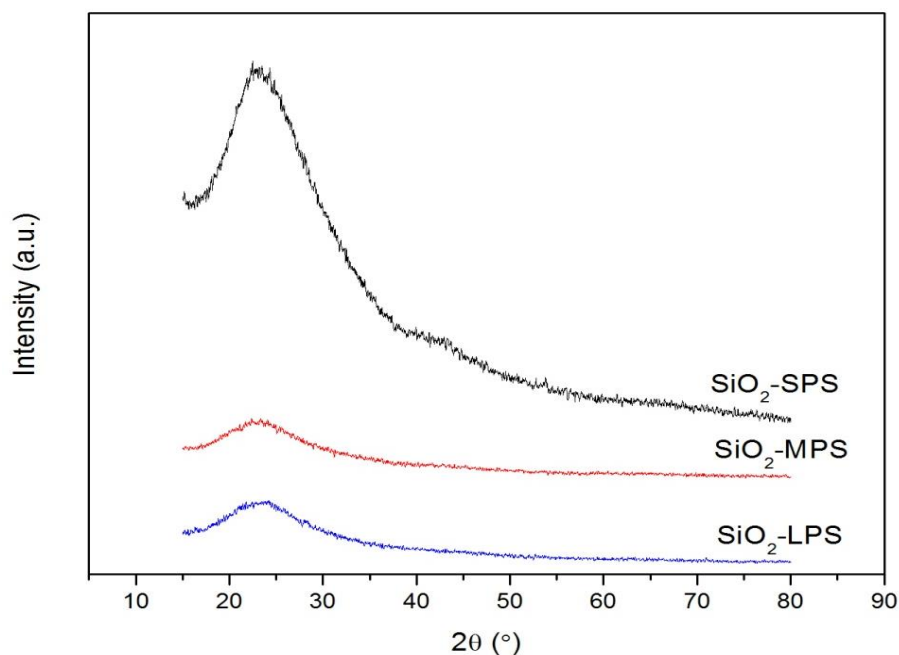


**Figure 4.1** XRD patterns of silica supports



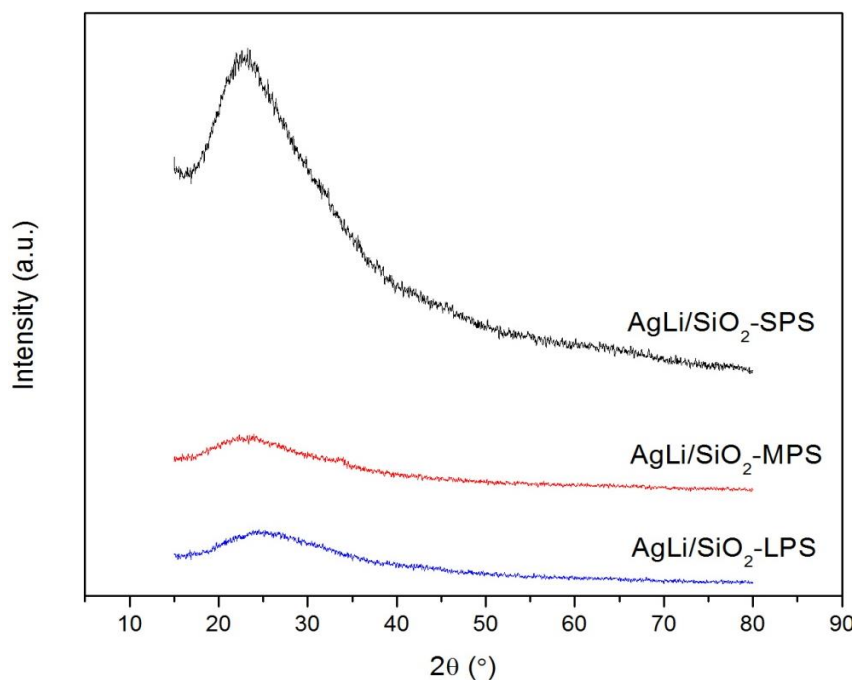


**Figure 4.2** XRD patterns of silver lithium supported on silica supports.

The structural properties of silica support and silver lithium catalysts were proven by XRD. Figures 4.1 and 4.2 showed the XRD patterns of all supports and catalysts, respectively. In this study, the XRD patterns of silica exhibited only amorphous form resulted in broad peak observation around 20-30°. The XRD patterns of silver lithium catalysts in Figure 4.2 were similar to the XRD patterns of silica support in Figure 4.1. This indicated that there is no presence of XRD patterns for silver and lithium due to the well dispersion of silver and lithium on the silica surface.

#### 4.1.1.2 Scanning electron microscopy (SEM) and energy dispersive X-ray spectroscopy (EDX)

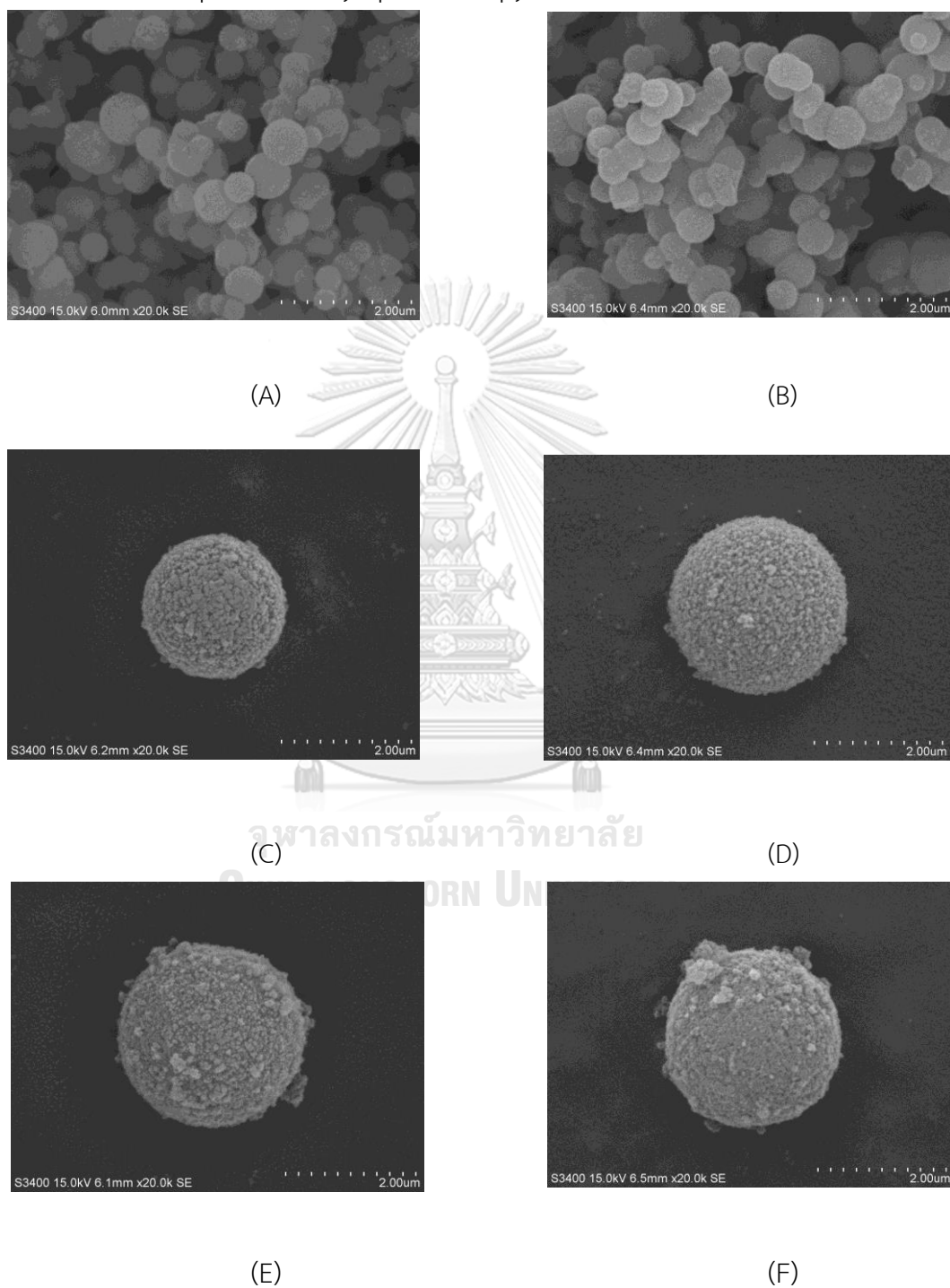


**Figure 4.3** The SEM images of catalysts (A) AgLi/SiO<sub>2</sub>-SPS, (B) SiO<sub>2</sub>-SSP, (C) AgLi/SiO<sub>2</sub>-MPS, (D) SiO<sub>2</sub>-MPS, (E) AgLi/SiO<sub>2</sub>-LPS, (F) SiO<sub>2</sub>-LPS

Figure 4.3 shows the morphology of supports and catalysts, which were studied using SEM. There is only a slight change of the morphology between supports and catalysts after the silver and lithium metal were impregnated into the silica particles. The addition of silver and lithium resulted in the increase of particles coating on the silica surface. It can be discussed that the loading of silver and lithium metals to the silica supports did not change the silica structure.

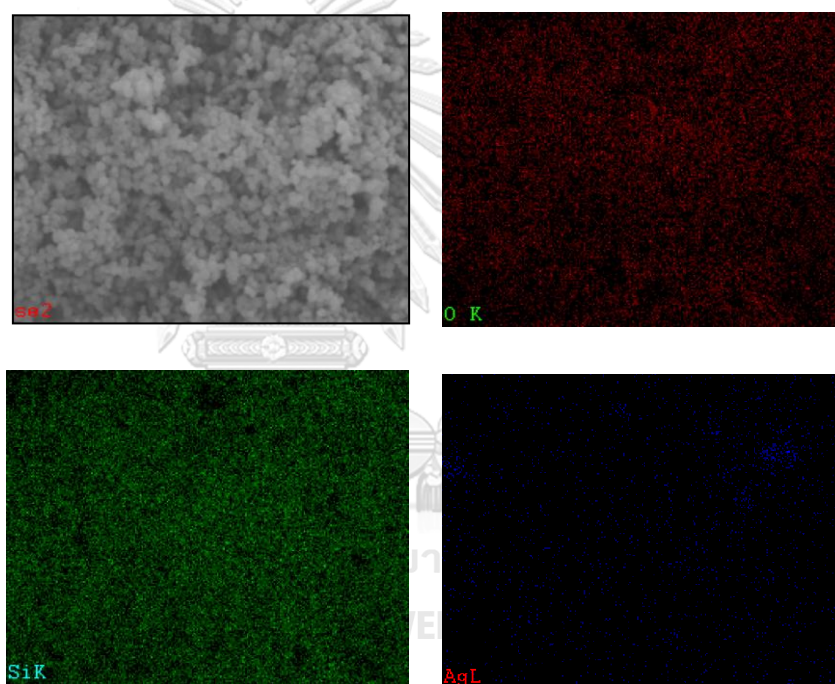


**Figure 4.4** EDX mapping of O (a), Si (b), and Ag (c) for AgLi/SiO<sub>2</sub>-SPS

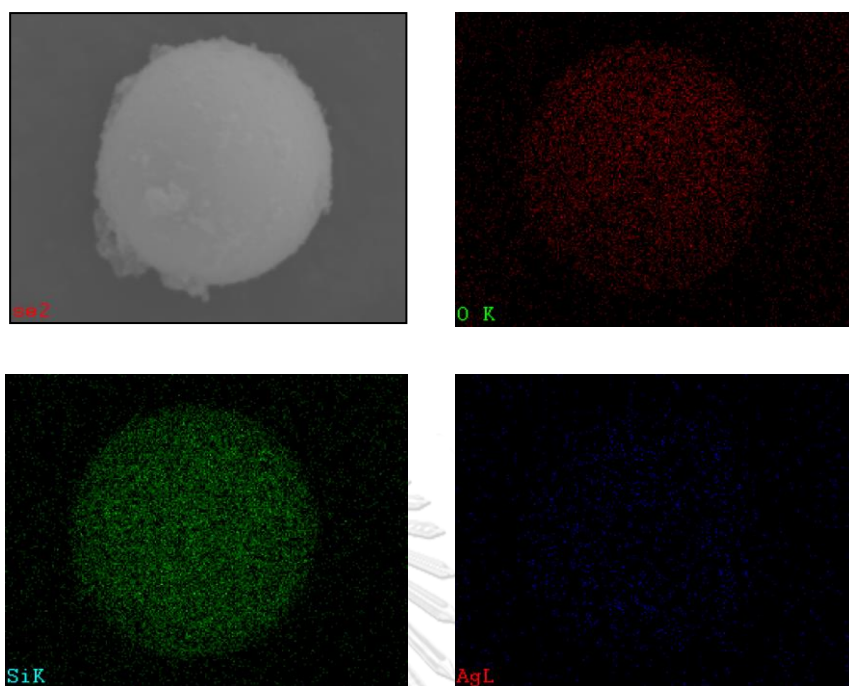


Figure 4.5 EDX mapping of O (a), Si (b), and Ag (c) for AgLi/SiO<sub>2</sub>-MPS

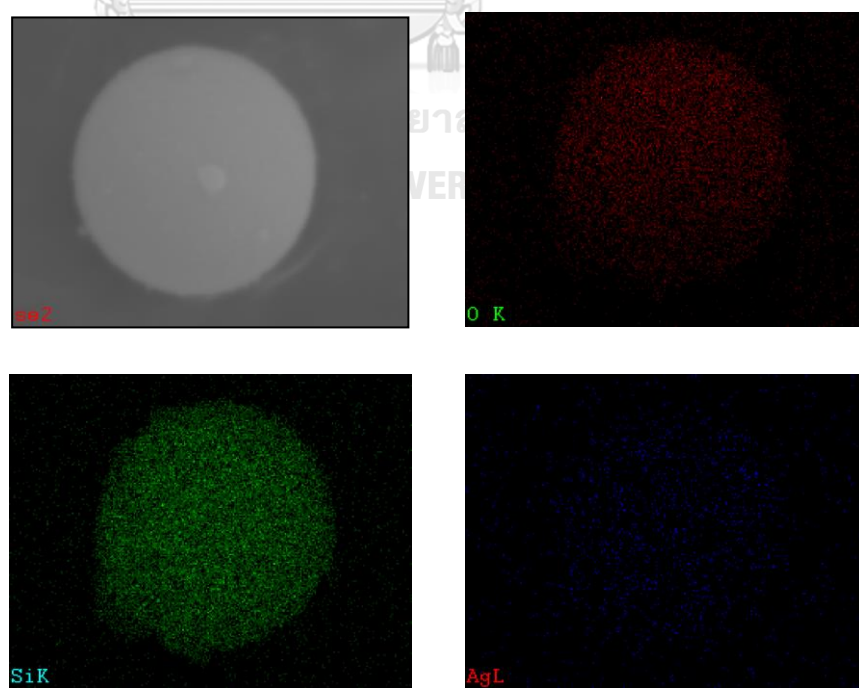


Figure 4.6 EDX mapping of O (a), Si (b), and Ag (c) for AgLi/SiO<sub>2</sub>-LPS

The results from the EDX mapping show the elemental distribution containing O (red), Si (green), and Ag (blue) dispersed on the catalyst surface (Figures 4.4-4.6). It can be observed that the silver species exhibit good dispersion on the silica support. In addition, the weight percentages of all elements are shown in the Table 4.1.

**Table 4.1** the elemental concentration of supports and catalysts determined by EDX

Catalysts	Wt%		
	Oxygen	Silicon	Silver
SiO <sub>2</sub> -SPS	38.8	61.2	-
SiO <sub>2</sub> -MPS	46.6	53.4	-
SiO <sub>2</sub> -LPS	44.8	55.2	-
AgLi/SiO <sub>2</sub> -SPS	42.5	52.0	5.5
AgLi/SiO <sub>2</sub> -MPS	51.6	43.1	5.3
AgLi/SiO <sub>2</sub> -LPS	45.3	49.3	5.4

As seen in Table 4.1, the weight percentage of silver for AgLi/SiO<sub>2</sub>-SPS, AgLi/SiO<sub>2</sub>-MPS, AgLi/SiO<sub>2</sub>-LPS were 5.5, 5.3, and 5.4 wt%, respectively. The weight percentage of each element from EDX is similar to the desired value in this experiment which are 4.7 wt% silver and 0.7 wt% lithium. It can be noted that there are a lot of metal near the surface of supports. From this EDX results, it showed that the silver metal has very well dispersion on the support surface that can increase the desired product yield [24-26]. This can also be confirmed the XRD results that there were the silver species on the supports.

#### 4.1.1.3 N<sub>2</sub>-physisorption

The results from N<sub>2</sub>-physisorption including BET surface area, pore volume and pore diameter of AgLi/SiO<sub>2</sub> are summarized in Table 4.2. It was found that all supports and catalysts exhibited microporous and mesoporous structure and their surface areas were remarkably high as expected. The BET surface area of silica supports decreased after the silver and lithium were impregnated into the supports. As a result, the surface area of SiO<sub>2</sub>-SPS decreased from 1023 to 675 after the addition of silver and lithium. Then, the surface area of AgLi/SiO<sub>2</sub>-SPS, AgLi/SiO<sub>2</sub>-MPS, and AgLi/SiO<sub>2</sub>-LPS were 675, 308, and 423 m<sup>2</sup>/g, respectively. Due to the AgLi/SiO<sub>2</sub>-SPS has the highest surface area, it can be suggested that AgLi/SiO<sub>2</sub>-SPS has well metal dispersion compared to AgLi/SiO<sub>2</sub>-MPS, and AgLi/SiO<sub>2</sub>-LPS catalysts.

**Table 4.2** The physical properties of SiO<sub>2</sub> and AgLi/SiO<sub>2</sub> catalysts

Entries	Catalyst	BET surface area (m <sup>2</sup> /g)	Pore volume (cm <sup>3</sup> /g)	Pore diameter (nm)	Particle size (micron)
1	SiO <sub>2</sub> -SSP	1023	0.90	2.0	0.6
2	SiO <sub>2</sub> -H52	521	1.60	9.8	2.0
3	SiO <sub>2</sub> -LPS	655	1.74	10.7	2.8
4	AgLi/SiO <sub>2</sub> -SPS	675	0.84	2.1	0.6
5	AgLi/SiO <sub>2</sub> -MPS	308	1.48	15.0	2.0
6	AgLi/SiO <sub>2</sub> -LPS	423	1.54	11.0	2.8

#### 4.1.2 Chemical properties characterization

#### 4.1.2.1 UV-visible spectroscopy (UV-vis)

The oxidation states of Ag were determined by UV-visible spectroscopy. The results are shown in Figure 4.7

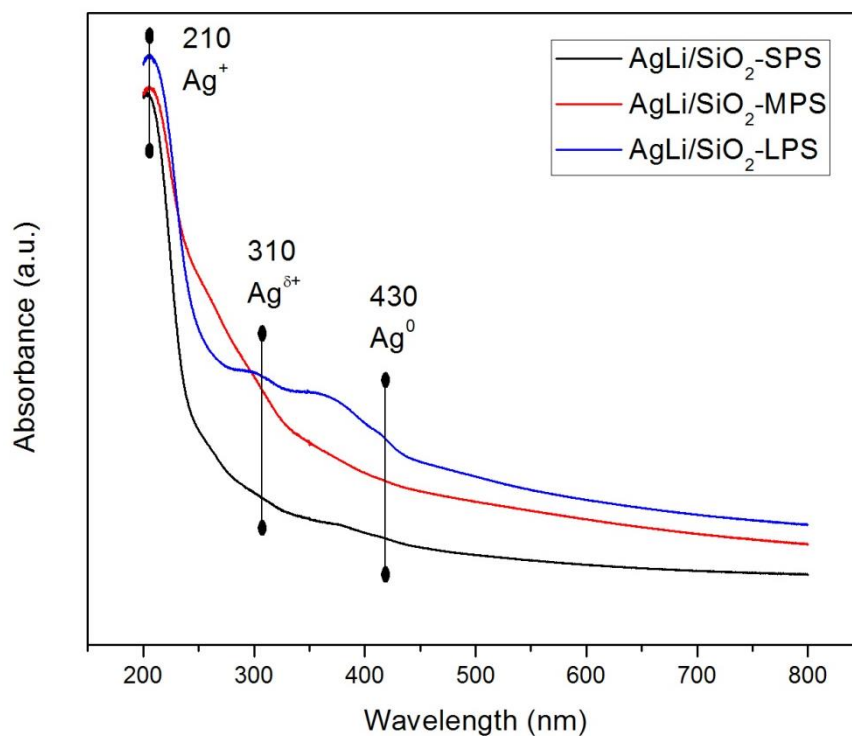


**Figure 4.7** The UV-visible spectra of all catalysts.

In the recent research, Janlamool et al. reported that the adsorption bands of  $\text{Ag}^+$ ,  $\text{Ag}_n^{\delta+}$  clusters, and  $\text{Ag}^0$  are around 210, 310, and 430 nm, respectively [9]. Figure 4.7 shows that  $\text{AgLi/SiO}_2\text{-LPS}$  exhibited the highest amount of  $\text{Ag}^+$ ,  $\text{Ag}_n^{\delta+}$  clusters, and metallic  $\text{Ag}^0$  species. Moreover, all silver species decreased in the following order:  $\text{AgLi/SiO}_2\text{-LPS} > \text{AgLi/SiO}_2\text{-MPS} > \text{AgLi/SiO}_2\text{-SPS}$ . In addition, A.N. Pestryakov et al. reported that  $\text{Ag}_n^{\delta+}$  ions are active states for partial oxidation of alcohol [27].

#### 4.1.2.2 Carbon dioxide temperature-programmed desorption (CO<sub>2</sub>-TPD)

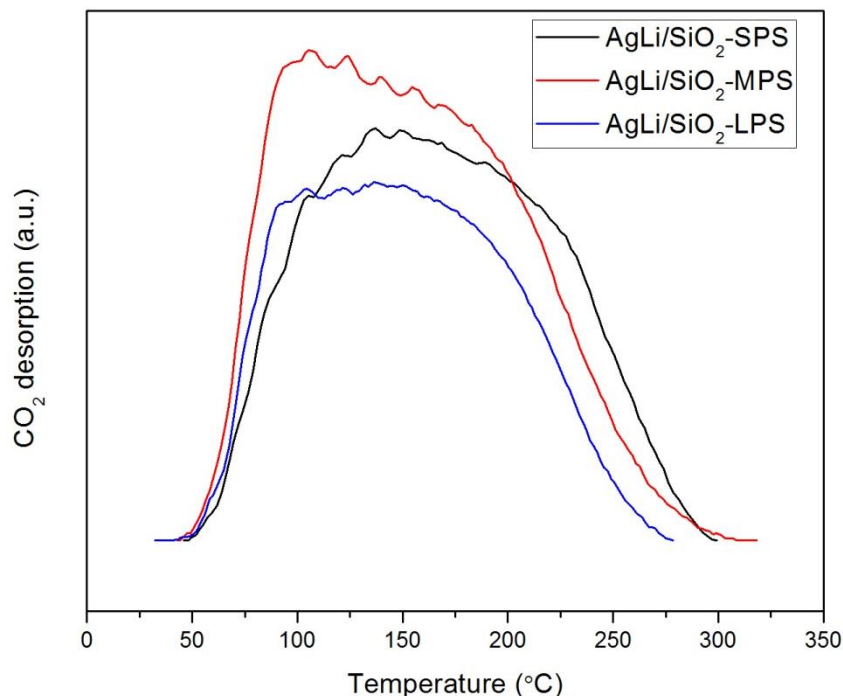


**Figure 4.8** CO<sub>2</sub>-TPD profiles of catalysts

This technique was used to determine the basicity of the catalysts. As seen in Figure 4.8, it can be observed that the CO<sub>2</sub>-TPD profiles were presented at the temperature ca. 50-300 °C. For more detail, the area under the curve of lower temperature peak is the amount of weak basic sites (50-150 °C) of catalysts and the area under the curve of higher temperature peak is the amount of moderate and strong basic sites (temperature > 150 °C) of catalysts [9, 28-30]. The results show that AgLi/SiO<sub>2</sub> catalysts mostly contained the weak basic sites. In addition, the amounts of basic sites of catalysts, which were obtained from CO<sub>2</sub>-TPD profiles are shown in Table 4.3.

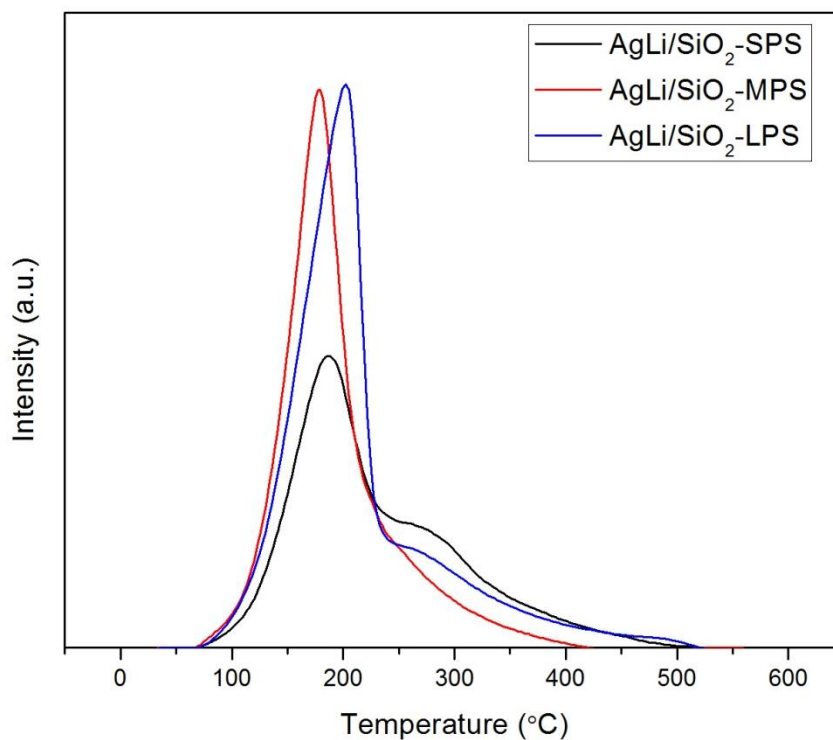


**Table 4.3** The amounts of basic sites of catalysts

Catalysts	The amounts of basic sites ( $\mu\text{mol CO}_2/\text{g cat}$ )		
	Weak basic sites	Moderate-Strong basic sites	Total basic sites
AgLi/SiO <sub>2</sub> -SPS	416.51	362.19	778.70
AgLi/SiO <sub>2</sub> -MPS	443.02	432.31	875.33
AgLi/SiO <sub>2</sub> -LPS	324.57	309.41	633.95

From Table 4.3, the amounts of total basic sites decreased in the following order of AgLi/SiO<sub>2</sub>-MPS > AgLi/SiO<sub>2</sub>-SPS > AgLi/SiO<sub>2</sub>-LPS. Moreover, the amounts of weak basic sites also decreased in the following order of AgLi/SiO<sub>2</sub>-MPS > AgLi/SiO<sub>2</sub>-SPS > AgLi/SiO<sub>2</sub>-LPS.

#### 4.1.2.3 Temperature-programmed reduction (H<sub>2</sub>-TPR)

**Figure 4.9** TPR profiles of catalysts.

The reducibility can be investigated by hydrogen temperature programmed reduction technique. This technique will be used when the characteristics of the sample are beyond the limitation of structural analysis detector such as X-ray diffraction. After all catalysts were prepared by incipient wetness impregnation method, they were analyzed by TPR and the results are shown in Figure 4.9. In fact, the TPR profiles depend on the parameters of catalyst such as metal-support interaction and metal particle size distribution [31, 32]. The TPR profiles of AgLi/SiO<sub>2</sub>-LPS and AgLi/SiO<sub>2</sub>-SPS displayed the narrow peak with shoulder, while the TPR peak of AgLi/SiO<sub>2</sub>-SPS was lower. However, only the narrow peak without shoulder was observed for the AgLi/SiO<sub>2</sub>-MPS catalyst. The TPR peaks with shoulder can be assigned to the overlap of two steps of silver reduction. The first step was assigned to the reduction of Ag<sup>+</sup> to Ag<sub>n</sub><sup>δ+</sup> clusters at the temperature range of 100 to 250 °C, while second step was defined to the reduction of Ag<sub>n</sub><sup>δ+</sup> clusters to Ag<sup>0</sup> at the temperature range of 250 to 330 °C.

4.2. Reaction test of the catalysts for non-oxidative dehydrogenation and oxidative dehydrogenation of ethanol.

#### 4.2.1. Non-oxidative dehydrogenation.

Reaction test of the catalysts for non-oxidative dehydrogenation was operated at atmospheric pressure and the temperature ranged from 200 to 400 °C. The catalyst was pre-reduced in flowing H<sub>2</sub> at 300 °C for 1 h prior to the vaporized ethanol was introduced into the reactor. The product distribution and ethanol conversion were investigated to consider the best condition for acetaldehyde formation. The results from catalytic study of

AgLi/SiO<sub>2</sub>-SPS, AgLi/SiO<sub>2</sub>-MPS, and AgLi/SiO<sub>2</sub>-LPS were shown in Figure 4.10-4.12 below.

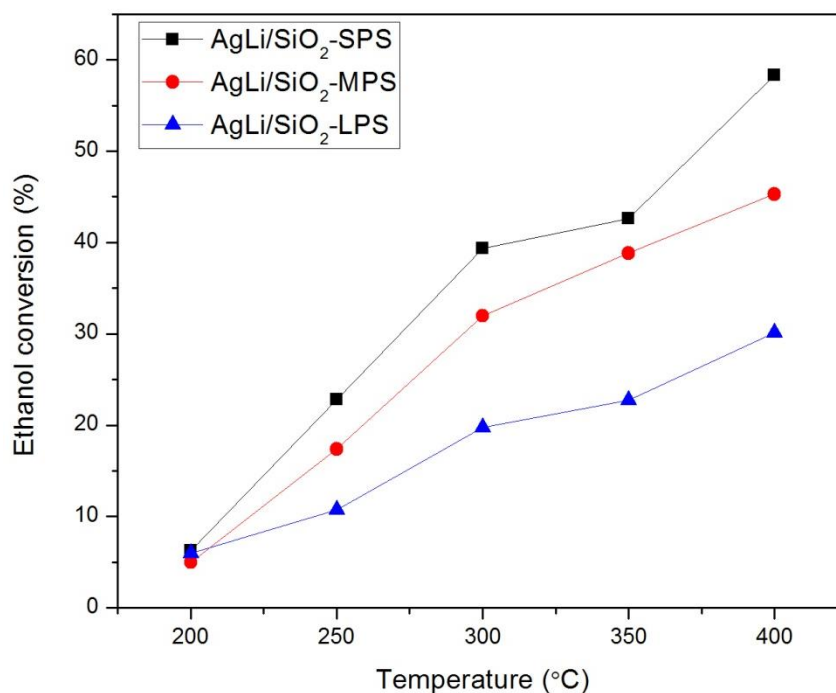


**Figure 4.10** Relation between ethanol conversion and temperature

From Figure 4.10, the results show that there is a relationship between ethanol conversion and temperature for all catalysts. The ethanol conversion increased when the temperature was raised. This relation associated with the endothermic nature of the dehydrogenation process that the endothermic reaction favors of high temperature [33]. The ethanol conversion at the temperature of 400 °C of the catalysts increased in the following order: AgLi/SiO<sub>2</sub>-SPS > AgLi/SiO<sub>2</sub>-MPS > AgLi/SiO<sub>2</sub>-LPS, where their values were 58.35, 45.29, and 30.12 %, respectively. The ethanol conversion corresponded to the amounts of weak basic sites from CO<sub>2</sub>-TPD, which play an important role of ethanol dehydrogenation

activity. The higher amount of weak basic sites led to the higher ethanol conversion [34, 35]. It can be observed that the larger amounts of weak basic sites for AgLi/SiO<sub>2</sub>-SPS and AgLi/SiO<sub>2</sub>-MPS provided the higher catalytic activity than AgLi/SiO<sub>2</sub>-LPS. However, there was another property, which led to the difference of ethanol conversion between AgLi/SiO<sub>2</sub>-SPS and AgLi/SiO<sub>2</sub>-MPS.

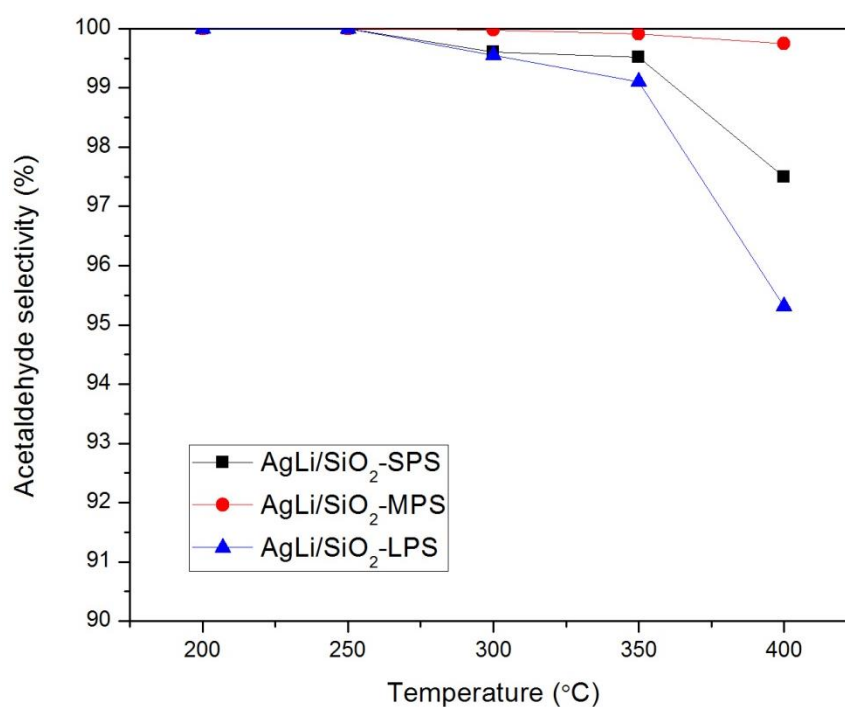


**Figure 4.11** Relation between acetaldehyde selectivity (%) and temperature (°C) for all catalyst

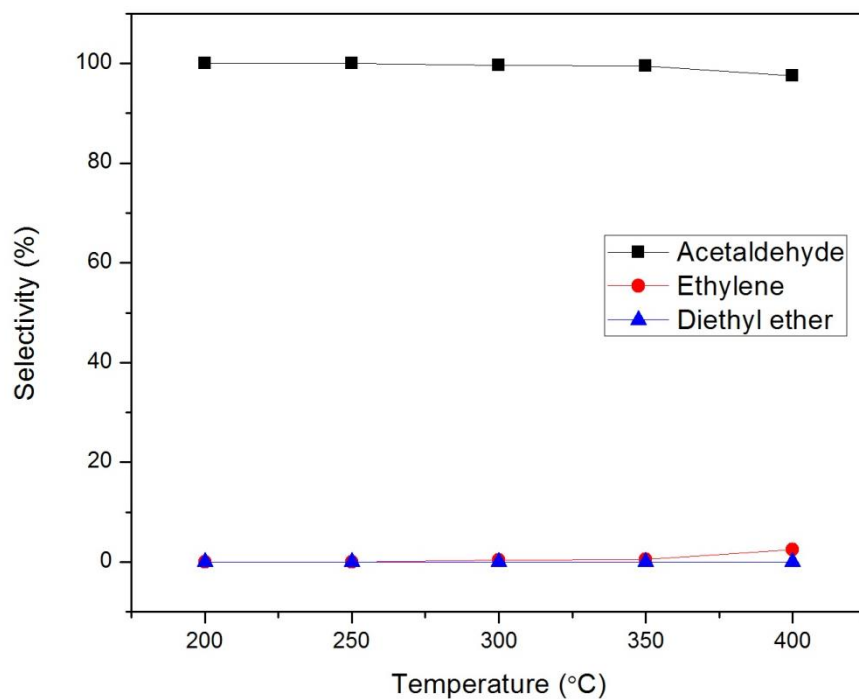


**Figure 4.12** Relation between product selectivity (%) and temperature (°C) for AgLi/SiO<sub>2</sub>-SPS catalyst

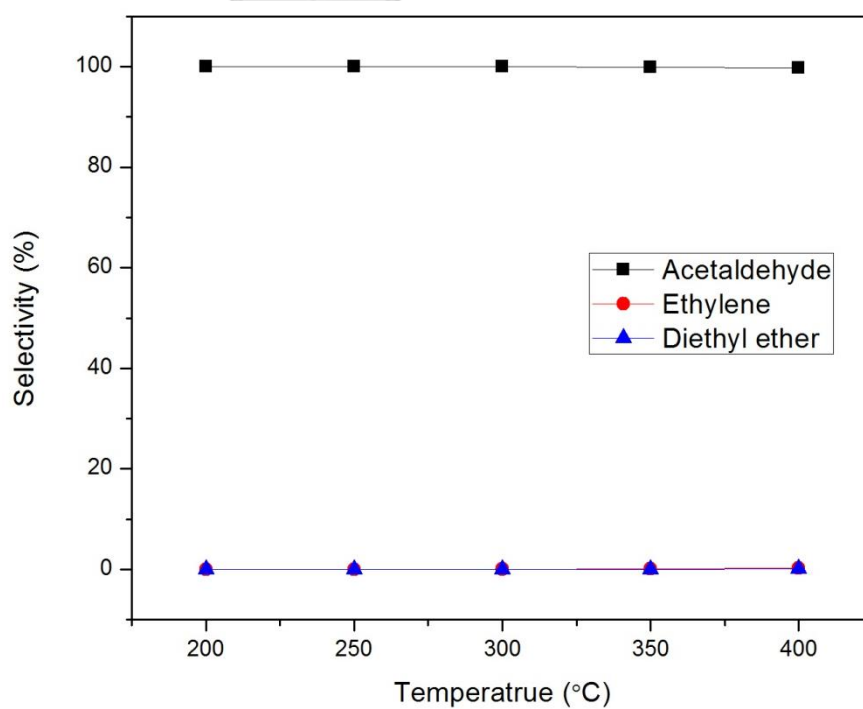


**Figure 4.13** Relation between product selectivity (%) and temperature (°C) for AgLi/SiO<sub>2</sub>-MPS catalyst

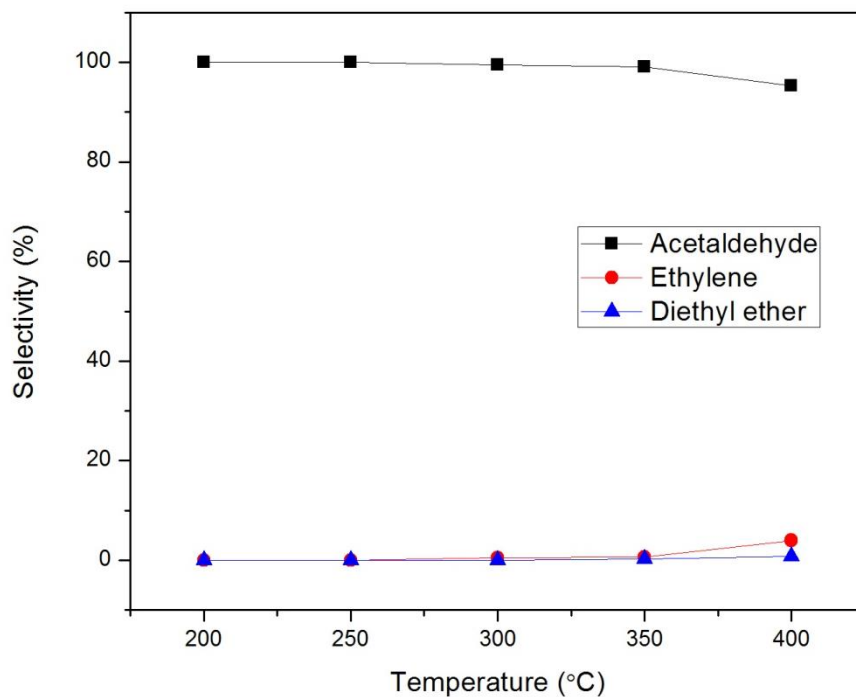


**Figure 4.14** Relation between product selectivity (%) and temperature (°C) for AgLi/SiO<sub>2</sub>-LPS catalyst

Figures 4.11-4.14 shows the product selectivity for all catalysts. The results showed that the acetaldehyde was a major product, which presented the selectivity of 100% at the reaction temperature around 200-250 °C. However, the slight decrease of acetaldehyde selectivity for all catalysts was observed due to the formation of ethylene and diethyl ether, while the reaction temperature was operated at higher than 250 °C.

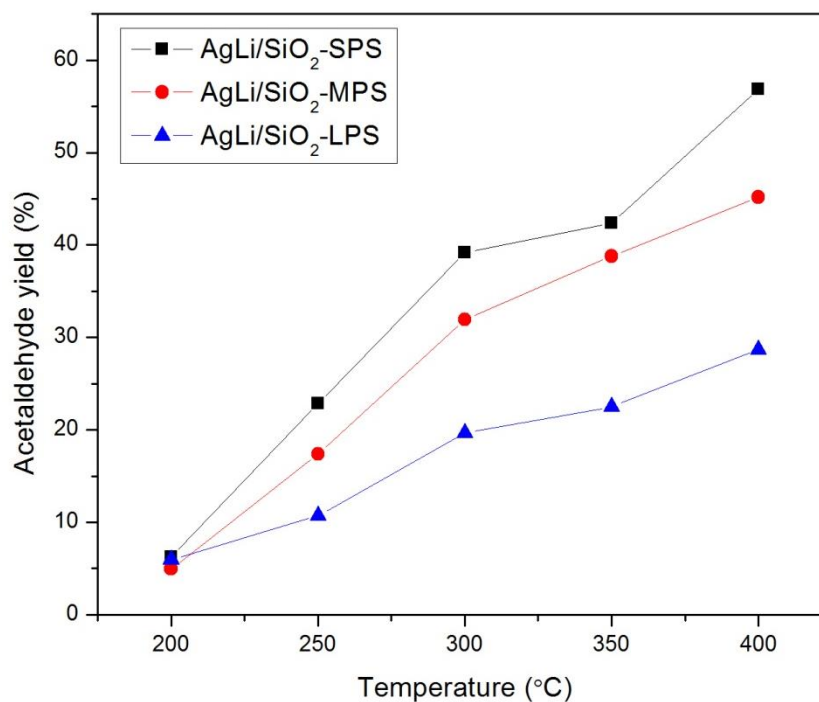


**Figure 4.15** Relation between acetaldehyde yield (%) and temperature (°C) for all catalysts

The relation between acetaldehyde yield and reaction temperature is shown in Figure 4.15. The results show that all catalysts have the similar trend of acetaldehyde yield, where the yields of acetaldehyde increased when the reaction temperature was raised. Moreover, the highest acetaldehyde yield of all catalysts was found at the temperature of 400 °C. AgLi/SiO<sub>2</sub>-SPS gave the highest acetaldehyde yield, which is around 57%. Thus, this catalyst is able to present the best catalytic performance for dehydrogenation of ethanol to acetaldehyde.

In order to illustrate the results from the non-oxidative dehydrogenation, summarized data is shown as seen in Table 4.4

**Table 4.4** The catalytic activity of all catalysts for non-oxidative dehydrogenation

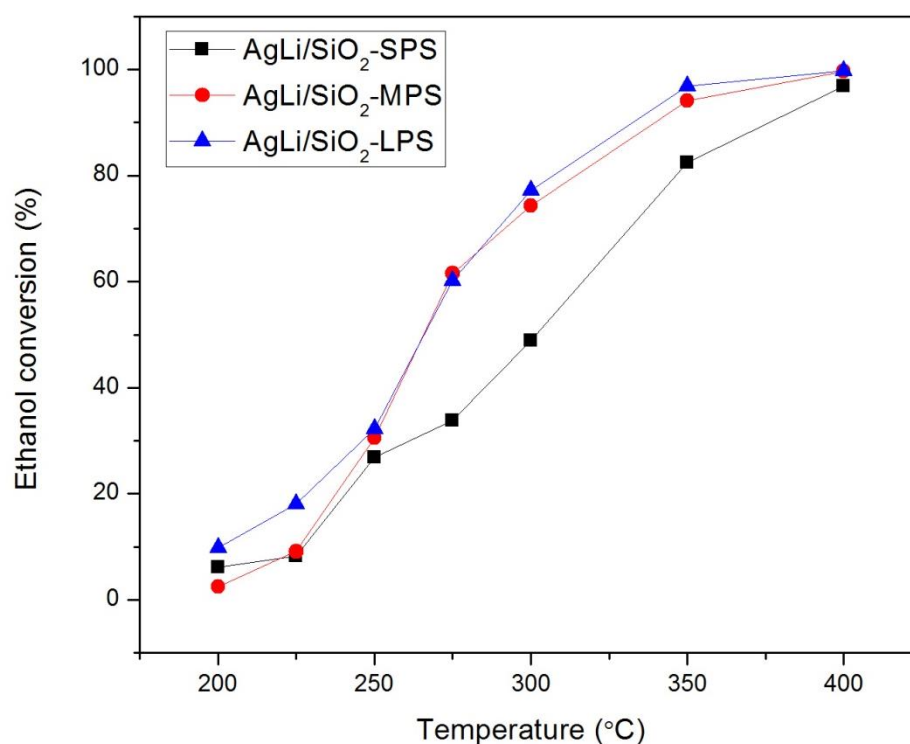
Catalyst	Temperature (°C)	Ethanol conversion (%)	Selectivity (%)			Acetaldehyde yield (%)
			Acetaldehyde	Ethylene	Diethyl ether	
AgLi/SiO <sub>2</sub> -SPS	200	6.23	100	-	-	6.23
	250	22.84	100	-	-	22.84
	300	39.36	99.61	0.39	-	39.21
	350	42.59	99.52	0.48	-	42.39
	400	58.35	97.50	2.50	-	56.89
AgLi/SiO <sub>2</sub> -MPS	200	4.97	100	-	-	4.97
	250	17.38	100	-	-	17.38
	300	31.95	99.98	0.02	-	31.94
	350	38.83	99.91	0.09	-	38.80
	400	45.29	99.75	0.25	0.06	45.18
AgLi/SiO <sub>2</sub> -LPS	200	5.97	100	-	-	5.97
	250	10.70	100	-	-	10.70
	300	19.76	99.55	0.45	-	19.67
	350	22.71	99.10	0.64	0.26	22.51
	400	30.12	95.31	3.96	0.73	28.71

#### 4.2.2. Oxidative dehydrogenation.

Reaction test of the catalysts for oxidative dehydrogenation was operated at atmospheric pressure and the temperature range from 200 to 400 °C. The reaction of oxidative



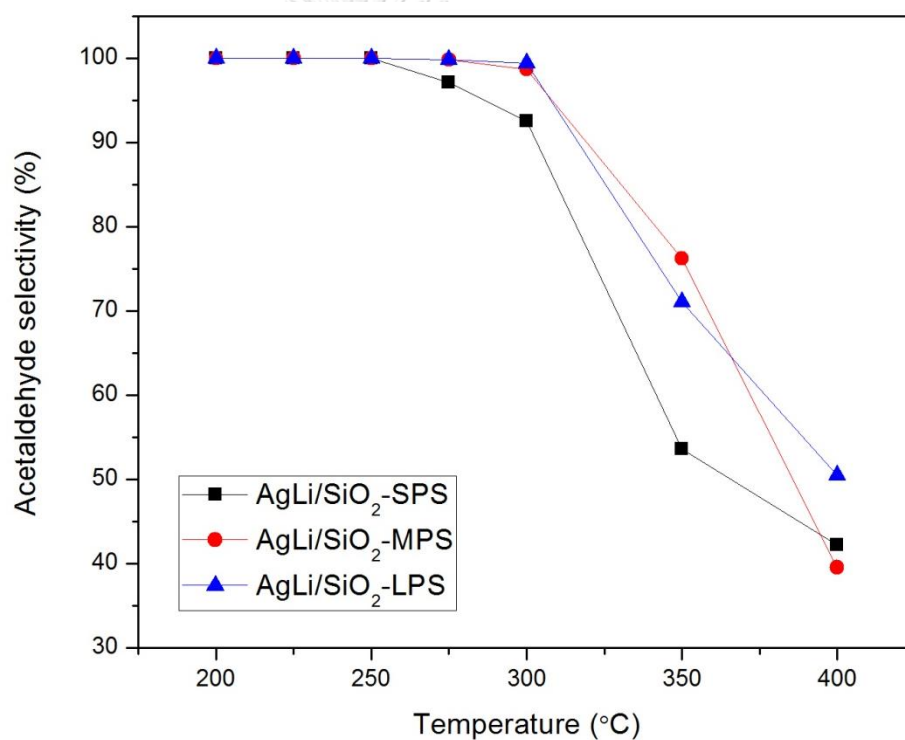
dehydrogenation was different from non-oxidative dehydrogenation due to the vaporized ethanol was mixed with oxygen before entering into the reactor. The results from catalytic test such as ethanol conversion, acetaldehyde selectivity, and acetaldehyde yield for oxidative dehydrogenation reaction are shown in Figures 4.16-4.21.



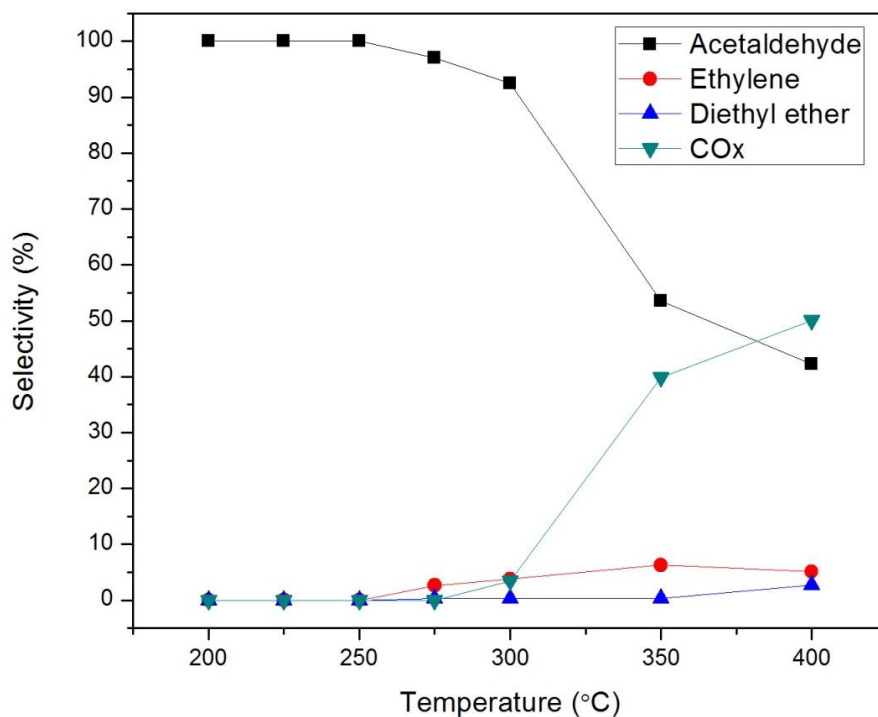
**Figure 4.16** Ethanol conversion of all catalysts for oxidative dehydrogenation reaction.

Figure 4.16 shows that the ethanol conversion of all catalysts increased when the reaction temperature was raised from 200 to 400 °C. The ethanol conversion of catalyst can be arranged in the order of: AgLi/SiO<sub>2</sub>-LPS > AgLi/SiO<sub>2</sub>-MPS > AgLi/SiO<sub>2</sub>-SPS. This results agree with the result from UV-visible technique. The amounts of Ag<sup>δ+</sup> clusters and Ag<sup>0</sup> were the key character for oxidative dehydrogenation [9, 27, 36]. In this study, the results showed that the catalytic activity corresponded to the amounts of

$\text{Ag}^{\delta+}$  clusters and  $\text{Ag}^0$  from UV-visible measurement, which are in the following order:  $\text{AgLi/SiO}_2\text{-LPS} > \text{AgLi/SiO}_2\text{-MPS} > \text{AgLi/SiO}_2\text{-SPS}$  and also be the same trend of the reducibility that is in the order of:  $\text{AgLi/SiO}_2\text{-LPS} > \text{AgLi/SiO}_2\text{-MPS} > \text{AgLi/SiO}_2\text{-SPS}$ . Moreover, it was also observed that the reducibility has the similar trend with catalytic activity. It can be suggested that the amount of  $\text{Ag}^{\delta+}$  clusters,  $\text{Ag}^0$ , and reducibility were important roles for ethanol conversion.



**Figure 4.17** Relation between acetaldehyde selectivity (%) and temperature (°C) for all catalysts



**Figure 4.18** Relation between product selectivity (%) and temperature (°C) for AgLi/SiO<sub>2</sub>-SPS catalyst

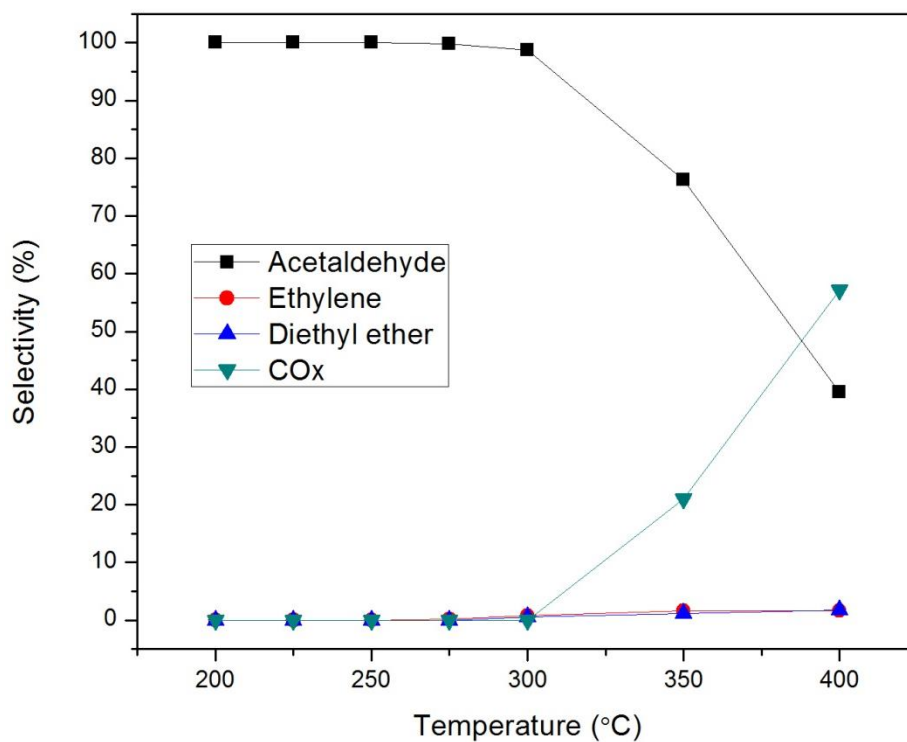


**Figure 4.19** Relation between product selectivity (%) and temperature (°C) for AgLi/SiO<sub>2</sub>-MPS catalyst

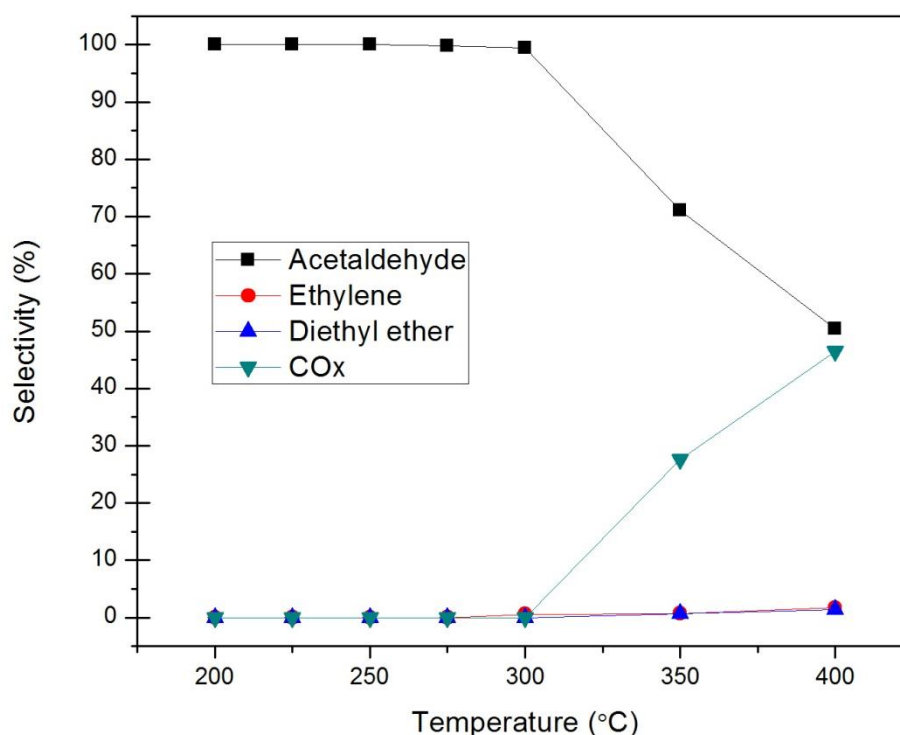


**Figure 4.20** Relation between product selectivity (%) and temperature (°C) for AgLi/SiO<sub>2</sub>-LPS catalyst

Figures 4.17-4.20 shows the selectivity of products. It can be observed that at low temperature (200-250 °C), the acetaldehyde was the main product having the selectivity of 100%. When the temperature was ranged from 275 to 300 °C, the acetaldehyde selectivity of all catalysts slightly decreased due to an existence of the by-products such as ethylene and diethyl ether for AgLi/SiO<sub>2</sub>-MPS and AgLi/SiO<sub>2</sub>-LPS. In addition, the small amount of CO<sub>2</sub> was observed for AgLi/SiO<sub>2</sub>-SPS. However, the acetaldehyde selectivity obviously decreased to 40-50% when the reaction temperature ranged from 350 to 400 °C. This was due to the large amounts of CO and CO<sub>2</sub> were produced as by-product at high temperature [9, 37, 38].

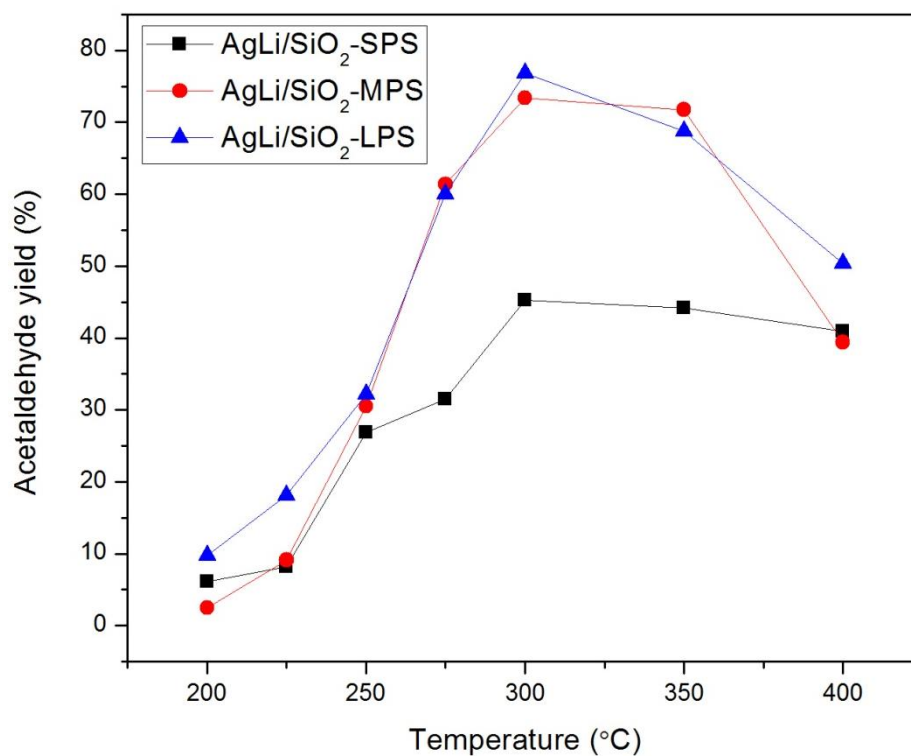


**Figure 4.21** acetaldehyde yield of all catalysts for oxidative dehydrogenation reaction.

Figure 4.21 shows the results of acetaldehyde yield for all catalysts. The highest value of acetaldehyde yield was at the temperature of 300 °C for all catalysts. It can be arranged in the order of AgLi/SiO<sub>2</sub>-LPS > AgLi/SiO<sub>2</sub>-MPS > AgLi/SiO<sub>2</sub>-SPS and their values were 76.81, 73.38, and 45.29%, respectively. Thus, AgLi/SiO<sub>2</sub>-LPS, which gave the highest acetaldehyde yield at 300°C, was suitable as the catalyst for oxidative dehydrogenation of ethanol to acetaldehyde.

In order to illustrate the results from the oxidative dehydrogenation, summarized data is shown as seen in Table 4.5

**Table 4.5** The catalytic activity of all catalysts for oxidative dehydrogenation

Catalyst	Temperature (°C)	Ethanol conversion (%)	Selectivity (%)					Acetaldehyde yield (%)
			Acetaldehyde	Ethylene	Diethyl ether	CO	CO <sub>2</sub>	
AgLi/SiO <sub>2</sub> -SPS	200	6.11	100	-	-	-	-	6.11
	225	8.22	100	-	-	-	-	8.22
	250	26.91	100	-	-	-	-	26.91
	275	33.85	97.09	2.64	0.27	-	-	32.86
	300	48.95	92.53	3.77	0.31	-	3.39	45.29
	350	82.41	53.57	6.27	0.36	18.42	21.38	44.15
	400	96.87	42.23	5.09	2.66	36.78	13.24	40.91
AgLi/SiO <sub>2</sub> -MPS	200	2.49	100	-	-	-	-	2.49
	225	9.11	100	-	-	-	-	9.11
	250	30.50	100	-	-	-	-	30.50
	275	61.51	99.81	0.19	-	-	-	61.39
	300	74.34	98.71	0.78	0.51	-	-	73.38
	350	94.13	76.21	1.60	1.18	20.17	0.84	71.74
	400	99.67	39.54	1.62	1.70	55.09	2.06	39.41
AgLi/SiO <sub>2</sub> -LPS	200	9.77	100	-	-	-	-	9.77
	225	18.09	100	-	-	-	-	18.09
	250	32.17	100	-	-	-	-	32.17
	275	60.17	99.82	-	-	-	-	60.06
	300	77.27	99.41	0.59	-	-	-	76.81
	350	96.85	71.05	0.71	0.69	14.41	13.14	68.81
	400	99.78	50.46	1.69	1.34	25.06	21.45	50.35

## CHAPTER 5

### CONCLUSIONS AND RECOMMENDATIONS

#### 5.1 Conclusions

This study represents the effect of different silica-supported silver-lithium catalysts via non-oxidative and oxidative dehydrogenation reactions of ethanol to acetaldehyde. Therefore, the results from the study can be concluded as follows:

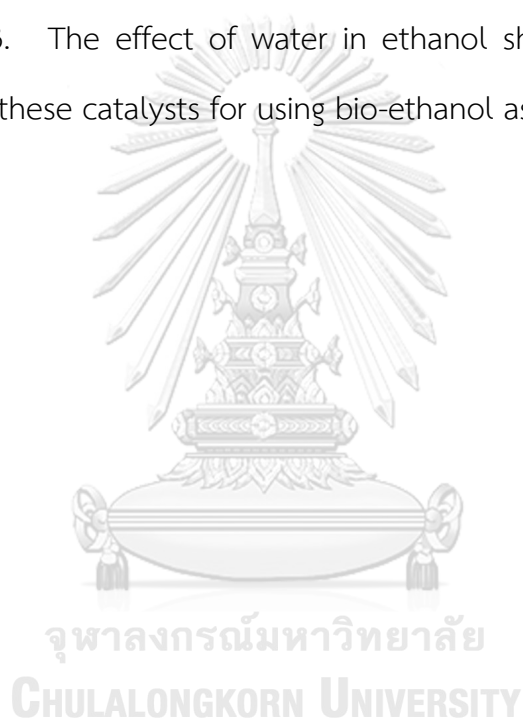
1. As seen the results in non-oxidative dehydrogenation, the weak basicity plays a strong influence. Therefore, AgLi/SiO<sub>2</sub>-SPS has the highest acetaldehyde yield due to its highest weak basicity among other catalysts.
2. As seen, the results in oxidative dehydrogenation, the amounts of Ag<sup>δ+</sup> clusters, Ag<sup>0</sup>, and reducibility are the important keys. As the results, AgLi/SiO<sub>2</sub>-LPS has the highest acetaldehyde yield at the reaction temperature of 300 °C.
3. The introducing of oxygen as the co-feed enhances the catalytic activity, which can be observed from the increasing of ethanol conversion.
4. The activity of the catalysts is not directly related to the particle size of silica.

## 5.2 Recommendations

1. The catalyst stability should be investigated in order to apply the good activity and stability of catalysts to the real use in industry.

2. The transmission electron microscopy (TEM) should be verified to confirm the morphologies such as metal dispersion.

3. The effect of water in ethanol should be investigated to apply these catalysts for using bio-ethanol as a starting material.





## REFERENCES

- [1] *Acetaldehyde Market*. Available:  
<https://www.mordorintelligence.com/industry-reports/acetaldehyde-market>
- [2] V. L. Sushkevich, I. I. Ivanova, and E. Taarning, "Mechanistic Study of Ethanol Dehydrogenation over Silica-Supported Silver," *ChemCatChem*, vol. 5, no. 8, pp. 2367-2373, 2013.
- [3] E. A. El-Sharkawy, S. S. Al-Shihry, and A. M. Youssef, "Structural characterization and catalytic activities of titania supported iron (III) oxide catalysts: Effect of Li<sup>+</sup> impregnation," *Materials Letters*, vol. 61, no. 14-15, pp. 2947-2951, 2007.
- [4] J. Sun and Y. Wang, "Recent Advances in Catalytic Conversion of Ethanol to Chemicals," *ACS Catalysis*, vol. 4, no. 4, pp. 1078-1090, 2014.
- [5] A. Neramittagapong, W. Attaphaiboon, and S. Neramittagapong, "Acetaldehyde Production from Ethanol over Ni-Based Catalysts," *Chiang Mai J. Sci*, vol. 35, pp. 171-177, 2008.
- [6] J. De Waele, V. V. Galvita, H. Poelman, C. Detavernier, and J. W. Thybaut, "PdZn nanoparticle catalyst formation for ethanol dehydrogenation: Active metal impregnation vs incorporation," *Applied Catalysis A: General*, vol. 555, pp. 12-19, 2018.
- [7] S.-i. Fujita, N. Iwasa, and H. Tani, "dehydrogenation of ethanol over cu-zno catalysts prepared from various coprecipitated precursors," *akadémiai kiadó*, vol. 73, no. 2, pp. 367-372, 2001.
- [8] V. V. K. e. al., *Redox mechanism for selective oxidation of ethanol over monolayer V2O5/TiO2 catalysts*. *Journal of catalysts*, 2016, p. 12.
- [9] J. Janlamool and B. Jongsomjit, "Oxidative dehydrogenation of ethanol over AgLi-Al<sub>2</sub>O<sub>3</sub> catalysts containing different phases of alumina," *Catalysis Communications*, vol. 70, pp. 49-52, 2015.

- [10] M. Eckert, G. Fleischmann, R. Jira, H. M. Bolt, and K. Golka, "Acetaldehyde," in *Ullmann's Encyclopedia of Industrial Chemistry*, 2006.
- [11] F.-W. Chang, H.-C. Yang, L. S. Roselin, and W.-Y. Kuo, "Ethanol dehydrogenation over copper catalysts on rice husk ash prepared by ion exchange," *Applied Catalysis A: General*, vol. 304, pp. 30-39, 2006.
- [12] Y. Guan and E. J. M. Hensen, "Ethanol dehydrogenation by gold catalysts: The effect of the gold particle size and the presence of oxygen," *Applied Catalysis A: General*, vol. 361, no. 1-2, pp. 49-56, 2009.
- [13] M. M. T. Khan, S. B. Halligudi, and S. Shukla, "Hydration of acetylene to acetaldehyde using  $K[Ru(III)(EDTA-H)Cl] \cdot 2H_2O$ ," *Journal of Molecular Catalysis*, vol. 58, pp. 299-305, 1990.
- [14] Y. Nishimura, M. Yamada, Y. Arikawa, T. Kamiguchi, T. Kuwahara, and H. Tanimoto, "Process for producing acetaldehyde," *United States Patent*, 1985.
- [15] "Chemical Economics Handbook," 2016.
- [16] X. J. e. al., "Silver/hydroxyapatite foam as a highly selective catalyst for acetaldehyde production via ethanol oxidation," *Catalysis Today*, 2016.
- [17] C. Wen, A. Yin, and W.-L. Dai, "Recent advances in silver-based heterogeneous catalysts for green chemistry processes," *Applied Catalysis B: Environmental*, vol. 160-161, pp. 730-741, 2014.
- [18] G. V. Mamontov, K. Sugino, and K. Sawabe, *Catalysis Today*, vol. 203, pp. 122-126, 2013.
- [19] G. V. Mamontov, M. V. Grabchenko, V. I. Sobolev, V. I. Zaikovskii, and O. V. Vodyankina, "Ethanol dehydrogenation over  $Ag-CeO_2/SiO_2$  catalyst: Role of  $Ag-CeO_2$  interface," *Applied Catalysis A: General*, vol. 528, pp. 161-167, 2016.
- [20] I. E. Wachs and R. J. Madix, "The oxidation of methanol on a silver (110) catalyst," *Surface Science*, vol. 76, pp. 531-558, 1978.
- [21] D. P. Volanti, "Insight into Copper-Based Catalysts: Microwave-Assisted Morphosynthesis, In Situ Reduction Studies, and Dehydrogenation of Ethanol," *ChemCatChem*, vol. 3, pp. 839-843, 2011.

- [22] J. Janlamool, P. Praserttham, and B. Jongsomjit, "Ti-Si composite oxide-supported cobalt catalysts for CO<sub>2</sub> hydrogenation," *Journal of Natural Gas Chemistry*, vol. 20, no. 5, pp. 558-564, 2011.
- [23] K. Fuchigami, Y. Taguchi, and M. Tanaka, "Synthesis of spherical silica particles by sol-gel method and application," *Polymers for Advanced Technologies*, vol. 19, no. 8, pp. 977-983, 2008.
- [24] M. Z. Jifeng Pand, Lei he, Lin Li, Xiaoli Pan, Aiqin Wang, *Upgrading ethanol to n-butanol over highly dispersed Ni-MgAlO catalysts*. *Journal of Catalysis* 2016, p. 10.
- [25] B. L. Pengyu Gong, Xianglong Kong, Jianjun Liu, Shengli Zuo, *Well-dispersed Ni nanoclusters on the surfaces of MFI nanosheets as highly efficient and selective catalyst for the hydrogenation of naphthalene to tetralin*. *Applied Surface Science*, 2017, p. 10.
- [26] A. A. Jalal Albadi, Mehdi Jalali, *Highly dispersed cobalt nanoparticles supported on a mesoporous Al<sub>2</sub>O<sub>3</sub>: An efficient and recyclable catalyst for aerobic oxidation of alcohols in aqueous media*. *Molecular Catalysis*, 2017, p. 7.
- [27] A.N.Pestryakov, *Alcohol selective oxidation over modified foam-silver catalysts*. *Catalysis Today*, 2004, p. 4.
- [28] X. Zhang, et al., "Effect of Ag promoter on redox properties and catalytic performance of Ag-Mo-PO catalysts for oxidative dehydrogenation of propane," *Applied Surface Science*, vol. 220, pp. 66-73, 2003.
- [29] e. a. Ruijuan Shi, *MgO-supported Cu nanoparticles for efficient transfer dehydrogenation of primary aliphatic alcohols*. *Catalysis Communications*, 2009, p. 4.
- [30] H. Bahruji, M. Bowker, C. Brookes, P. R. Davies, and I. Wawata, "The adsorption and reaction of alcohols on TiO<sub>2</sub> and Pd/TiO<sub>2</sub> catalysts," *Applied Catalysis A: General*, vol. 454, pp. 66-73, 2013.
- [31] T. F. F. Pinna, G. Strukul, "TPR and XRD study of ammonia synthesis catalysts," *Applied Catalysis A: General*, vol. 149, pp. 341-351, 1997.

- [32] D. Chen *et al.*, "Comparative studies of silver based catalysts supported on different supports for the oxidation of formaldehyde," *Catalysis Today*, vol. 175, no. 1, pp. 338-345, 2011.
- [33] J. M. C. a. H. K. Joshi, *Acetaldehyde by Dehydrogenation of Ethyl Alcohol*. Industrial And Engineering Chemistry, 1951, p. 8.
- [34] S. Cimino, L. Lisi, and S. Romanucci, "Catalysts for conversion of ethanol to butanol: Effect of acid-base and redox properties," *Catalysis Today*, vol. 304, pp. 58-63, 2018.
- [35] S. Colley, J. Tabatabaei, K. Waugh, and M. Wood, "The detailed kinetics and mechanism of ethyl ethanoate synthesis over a Cu/Cr<sub>2</sub>O<sub>3</sub> catalyst," *Journal of Catalysis*, vol. 236, no. 1, pp. 21-33, 2005.
- [36] A.N.Pestryakov, "modification of silver catalysts for oxidation of methanol to formaldehyde," *Catalysis Today*, vol. 28, pp. 239-244, 1996.
- [37] W. Chatkaew, "Oxidative dehydrogenation of ethanol to acetaldehyde over AgLi/TiO<sub>2</sub> Catalyst," Master, Chemical Engineering, Chulalongkorn University, 2017.
- [38] N. Sukarawan, "Oxidative dehydrogenation of ethanol over Cu-AgLi/Al<sub>2</sub>O<sub>3</sub> Catalysts," Master, Chemical Engineering, Chulalongkorn University, 2016.



## APPENDIX A

## CALCULATION OF CATALYST PREPARATION

The catalysts were synthesized by incipient wetness co-impregnation method for silver-lithium catalysts supported on different silica. The calculation of the preparation are showed as follows:

<b>Reagent:</b>	-	Silver (I) nitrate ( $\text{AgNO}_3$ )	
		Molecular weight	= 169.87 g/mol
		Silver (Ag) atomic weight	= 107.87 g/mol
	-	Lithium (I) nitrate ( $\text{LiNO}_3$ )	
		Molecular weight	= 68.95 g/mol
		Lithium (Li) atomic weight	= 6.94 g/mol
<b>Calculation:</b>	Based on 1 g of catalyst, so Ag 4.7%	=	0.047 g
	Li 0.7%	=	0.007 g
	$\text{SiO}_2$ support	=	$1 - (0.047 + 0.007) = 0.946$ g

For all catalysts:  $\text{AgLi/SiO}_2$

$$\text{SiO}_2 \text{ support} = 1 - (0.047 + 0.007) = 0.946 \text{ g}$$

There is 107.87 g of Ag in 169.87 g of  $\text{AgNO}_3$  reagent

So, 0.047 g of Ag is from 0.074 g of  $\text{AgNO}_3$  reagent

There is 6.94 g of Li in 68.95 g of  $\text{LiNO}_3$  reagent

So, 0.007 g of Li is from 0.0695 g of  $\text{LiNO}_3$  reagent

## APPENDIX B

### CALIBRATION CURVES

The composition and retention time of reactants, main product and by products gas were analyzed by a Shimadzu GC14B (DB5) gas chromatograph equipped with FID and a Shimadzu GC8A (molecule sieve 5A and Parapak Q) gas chromatography equipped with TCD

The chromatogram distinguishes retention times of reactant, main product, and by product

**Table B1** Retention times of reactant for FID and TCD gas chromatography

Chemicals	Detector of GC	Retention time in GC
Ethanol	FID	4.6
Acetaldehyde	FID	4.3
Ethylene	FID	4.1
Diethyl Ether	FID	4.9
Carbon Monoxide	TCD	4.8
Carbon Dioxide	TCD	2.5

The calibrate curves were used for evaluating the mole of ethanol as a reactant gas, acetaldehyde as a main product, and ethylene, diethyl ether, CO and CO<sub>2</sub> as by products in both of oxidative dehydrogenation and dehydrogenation reactions. The calibration curves of their chemicals are illustrated in Figure C.1-C.6

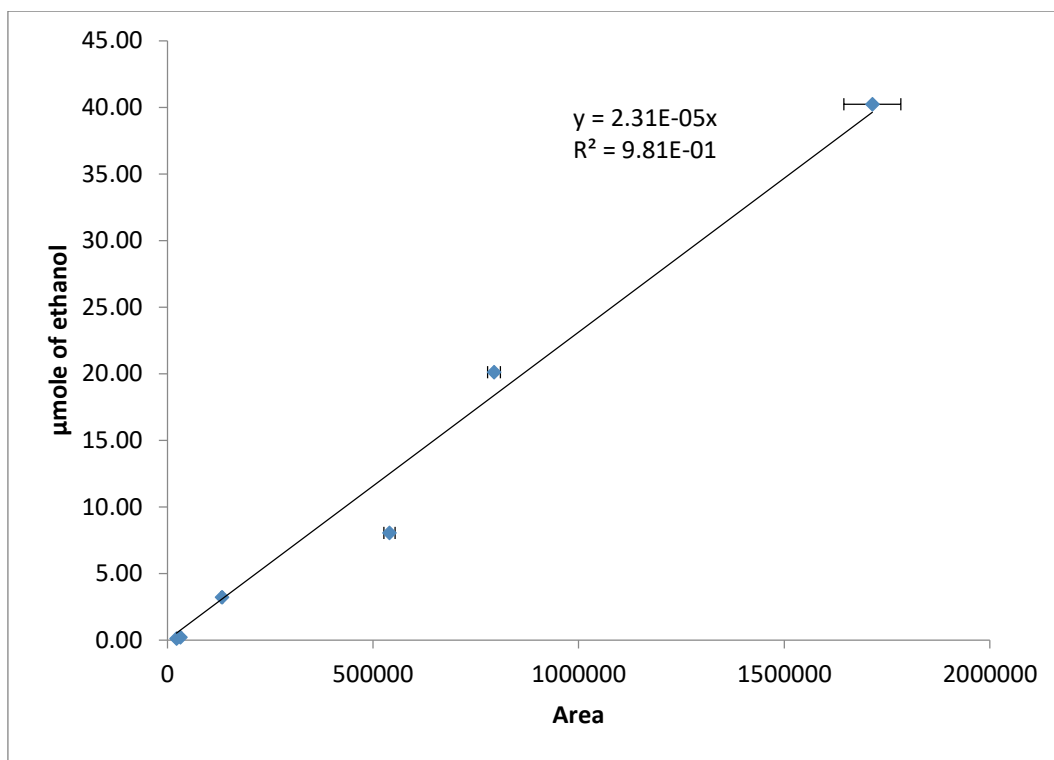


Figure B.1 The calibration curve of ethanol

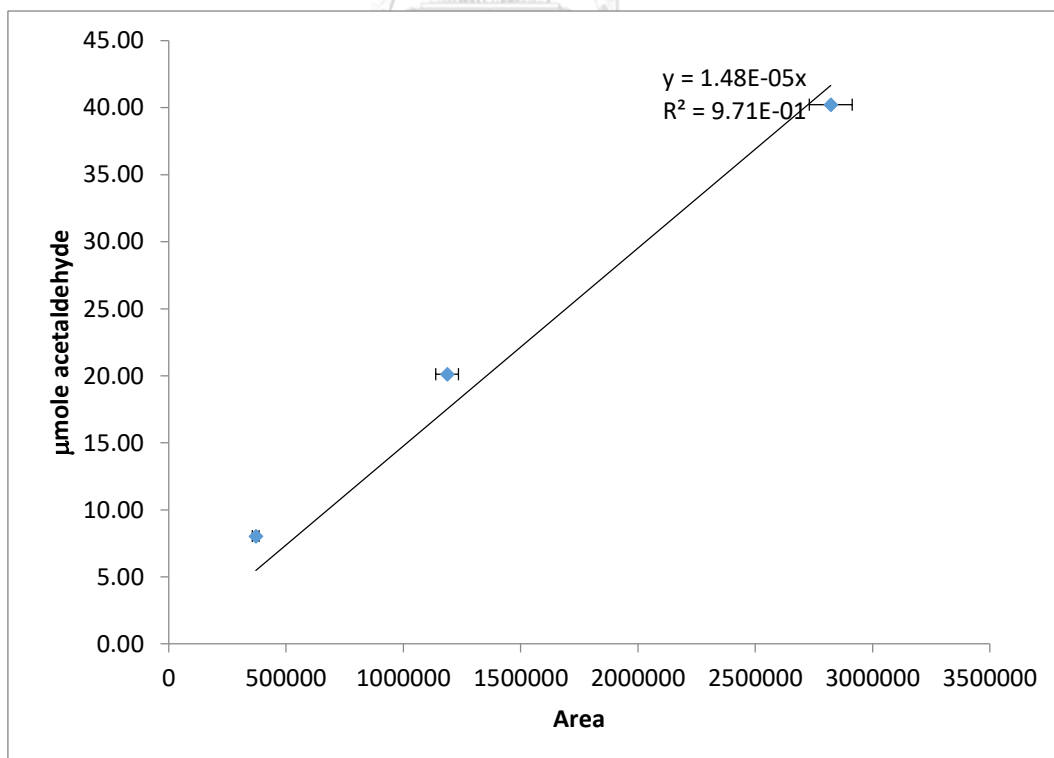


Figure B.2 The calibration curve of acetaldehyde



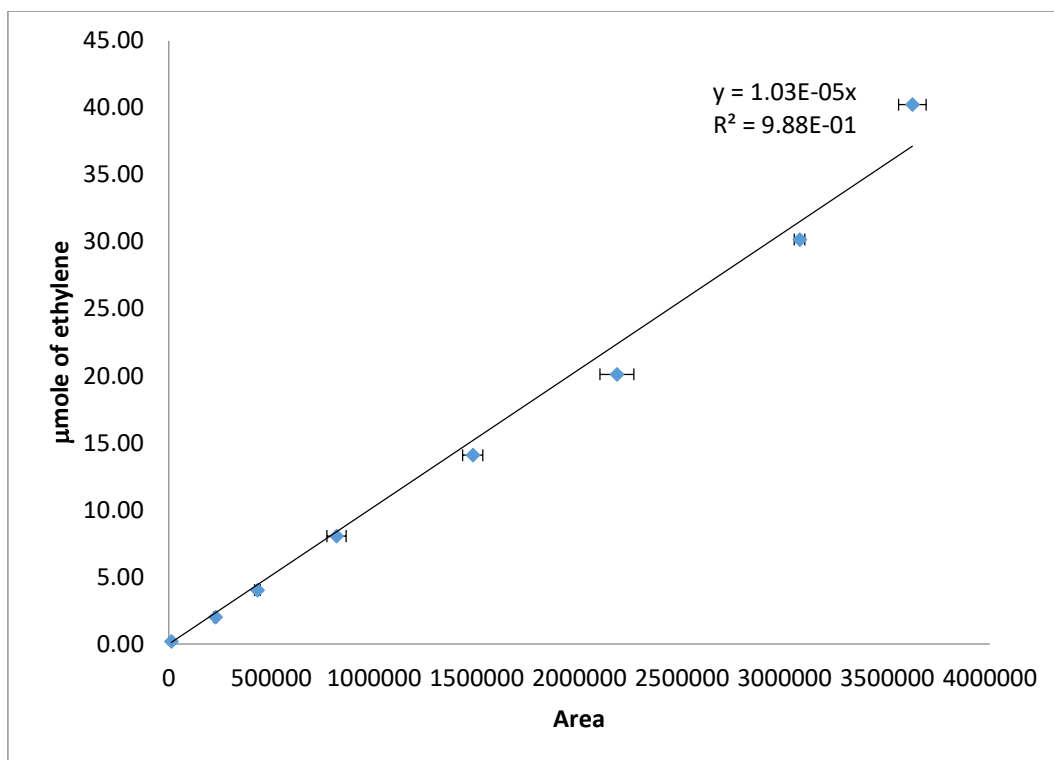


Figure B.3 The calibration curve of ethylene

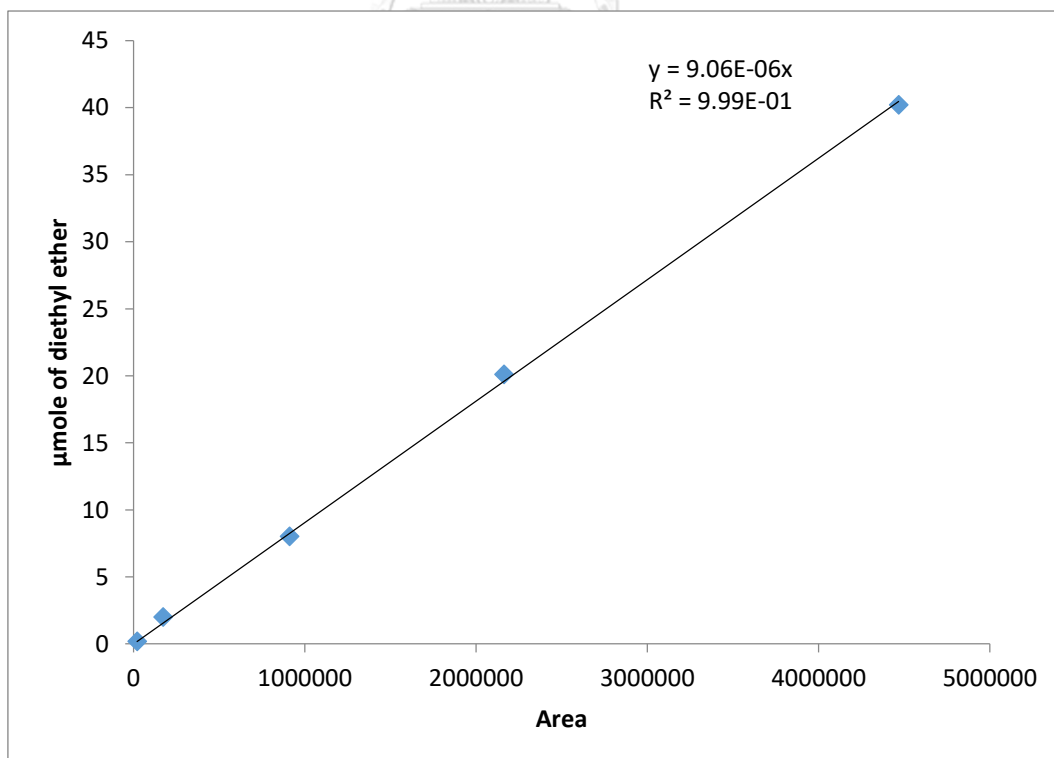


Figure B.4 The calibration curve of diethyl ether

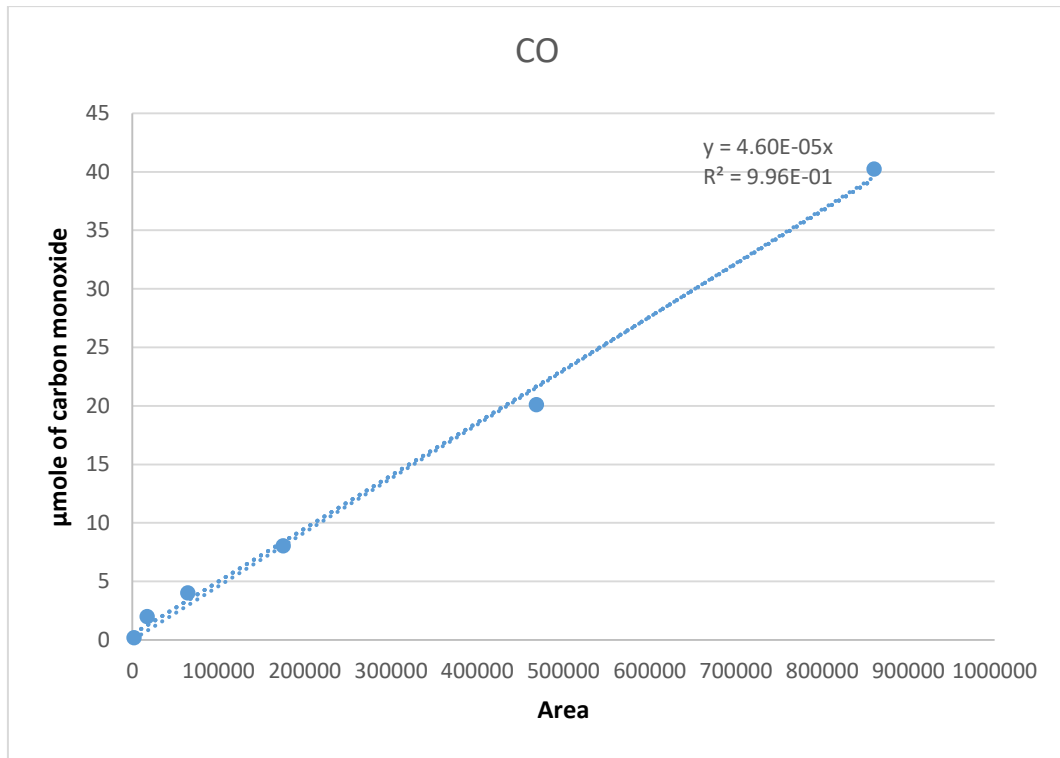


Figure B.5 The calibration curve of carbon monoxide

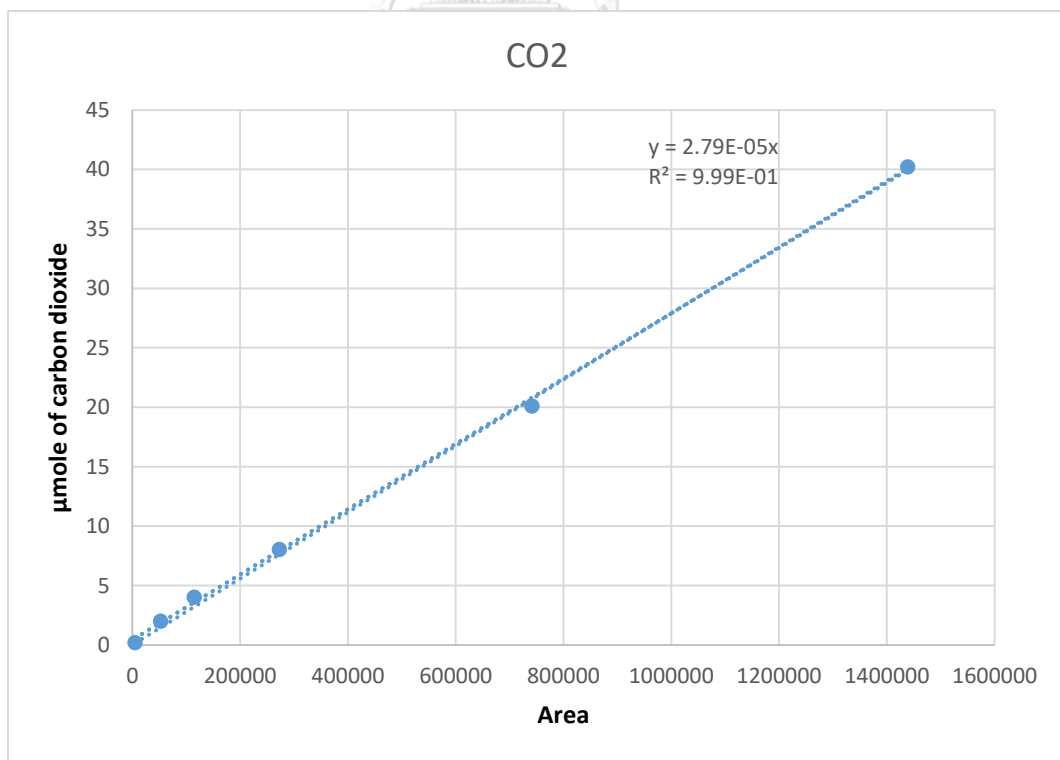


Figure B.6 The calibration curve of carbon dioxide

## APPENDIX C

## CALCULATION OF TOTAL BASIC SITES OF CATALYSTS

The surface basicity and strength of basic site for catalysts can be computed from the CO<sub>2</sub> - TPD profiles by following these steps

Definition – the area of the CO<sub>2</sub> – TPD profiles of each sample = A

The mole of CO<sub>2</sub> was determined from the calibration curve of CO<sub>2</sub> desorbed as following formula:

The mole of CO<sub>2</sub> (μmole) = 17.624 x A

Definition – Amount of each sample = B g

The amount of basic sites of sample was determined in the range of temperature by this formula:

$$\begin{aligned} \text{The basicity of sample } (\mu\text{mole CO}_2/\text{g cat}) &= \frac{\mu\text{mole of CO}_2 \text{ of the sample}}{\text{Amount of dry catalysts}} \\ &= \frac{17.624 \times A}{B} \end{aligned}$$

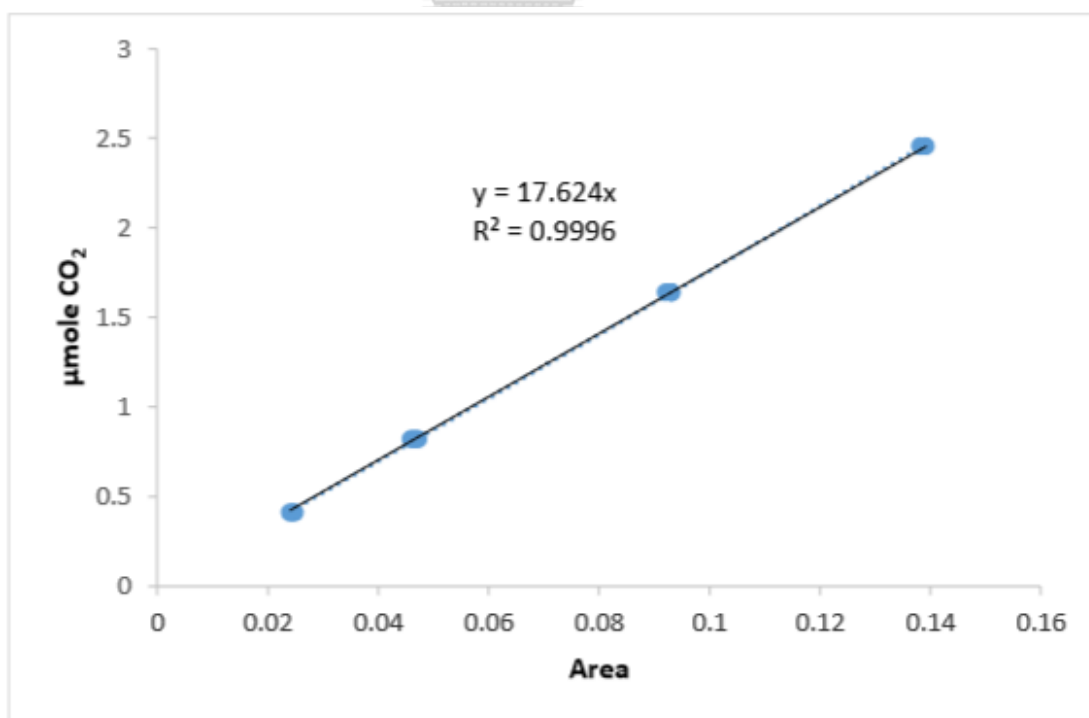


Figure C.1 The calibration curve of carbon dioxide obtained from CO<sub>2</sub> – TPD profiles

## APPENDIX D

## CALCULATION OF CONVERSION, SELECTIVITY AND YIELD

The ethanol conversion was calculated as defined equations as follows:

$$\text{Conversion (\%)} = \frac{(\text{mole of ethanol feed} - \text{mole of ethanol reacted}) \times 100}{\text{mole of ethanol feed into the reactor}}$$

The activity of the catalysts in oxidative dehydrogenation and dehydrogenation reactions can be estimated by 2 choices; the first one is from the selectivity that defined as the moles of products formed with respect to total moles of all products, and another one is from the yield that defined as the results of selectivity and conversion. The selectivity and the yield were calculated as equations as follow:

$$\text{Acetaldehyde selectivity (\%)} = \frac{\text{mole of acetaldehyde produced} \times 100}{\text{mole of all products produced}}$$

$$\text{Acetaldehyde yield (\%)} = \frac{\text{selectivity of acetaldehyde} \times \text{conversion}}{100}$$



จุฬาลงกรณ์มหาวิทยาลัย  
**CHULALONGKORN UNIVERSITY**

## VITA

Mr. Narawich Mukda was born on September 28th, 1993 at Sriracha hospital, Chonburi provine, Thailand. He finished high school from Rayongwittayakom School in 2011 and graduated in Bachelor's degree from Department of Chemical Engineering, Faculty of Engineering, King Mongkut's University of Technology Thonburi, Thailand in July 2016. He has further studied in Master's degree at Department of Chemical Engineering, Faculty of Engineering, Chulalongkorn University since August 2016.





จุฬาลงกรณ์มหาวิทยาลัย  
**CHULALONGKORN UNIVERSITY**